

WISCONSIN HIGHWAY RESEARCH PROGRAM #0092-06-05

**COMPARISON OF BASIC LABORATORY TEST RESULTS WITH MORE
SOPHISTICATED LABORATORY AND IN-SITU TESTS METHODS ON
SOILS IN SOUTHEASTERN WISCONSIN**

FINAL REPORT

Principal Investigators: Tuncer B. Edil and Craig H. Benson

Research Associates: Lin Li, David Mickelson, Felipe F. Camargo

Geo Engineering Program
Department of Civil and Environmental Engineering
University of Wisconsin-Madison

SUBMITTED TO THE WISCONSIN
DEPARTMENT OF TRANSPORTATION

March 21, 2009

EXECUTIVE SUMMARY

This report describes a comparison of basic laboratory test results with more sophisticated laboratory and in situ tests methods on soils in Southeastern Wisconsin. The generated soils data in the Milwaukee Marquette Interchange project has been used in an attempt to correlate the more 'routine' laboratory tests to determine geotechnical design parameters (such as phi-angle, cohesion, unit weight, unconfined compression, consolidation characteristics, etc.). Correlations were identified among undrained shear strength, cohesion, friction angle, consolidation parameters, soil type, Atterberg limits, effective normal stress, and geological origin. ANOVA and non-linear regression techniques were applied to identify and develop correlation equations. Regression analysis found that the undrained shear strength (S_u) exponentially decreases with liquidity index and liquid limit. The S_u/σ_z' exponentially decreases with liquidity index and S_u/σ_z' is constant over liquid limit and preconsolidation stress σ_c' ($S_u/\sigma_z' = 0.22$). The S_u/σ_z' can be linearly expressed by plasticity index and expressed by OCR with a power function. The relationship among S_u/σ_z' and LI, LL, PI, OCR, and σ_c' are close to the published correlation in the literature. Mean value (0.2) of c'/σ_z' measured by CU triaxial tests is very close to reported value in the literature. Data of $\sin\phi'$ and plasticity index are distributed around the published linear relationship between $\sin\phi'$ and $\ln(\text{PI})$. The data of c'/σ_z' and PI also support the published linear relationship between c'/σ_z' and PI. Compression index (C_c) and swell index (C_s) data are correlated as $C_s \approx 0.2$ to $0.1 C_c$. The data of C_c is linearly varied with liquid limit and in situ void ratio. The S_u data are related to SPT N as a function of soil type. These relationships are intended to assist the engineers to estimate structural properties based on geological origin and simpler index tests such as Atterberg limits. In planning stages, they provide valuable estimates of structural properties for analysis. It further allows verification of structural test results when become available as to their reasonableness in comparison to the historical data.

ACKNOWLEDGEMENT

Financial support for this study was provided by the Wisconsin Highway Research Program. The conclusions and recommendations in this report are solely those of the authors and do not reflect the opinions or policies of the Program. Steve Maxwell provided the data and the related reports of the project.

TABLE OF CONTENTS

EXECUTIVE SUMMARY	i
ACKNOWLEDGEMENT	ii
LIST OF TABLES	iv
LIST OF FIGURES	v
1. INTRODUCTION	1
2. RESEARCH OBJECTIVE.....	2
3. BACKGROUND.....	2
4. MAIN APPROACH.....	5
4.1 Compilation of Data in Electronic Media	5
4.2 Identification of Potential Correlations	7
4.3 Statistical Analysis and Interpretation	8
5. RESULTS AND DISCUSSIONS	9
5.1 Geological Origin	9
5.2 Strength	11
5.3 Compression	18
5.4 Field Test	20
6. CONCLUSIONS	21
7. RECOMMENDATIONS	24
8. REFERENCES.....	26
TABLES	28
FIGURES.....	31
APPENDICES.....	64

LIST OF TABLES

Table 1. Properties of subgrade soils.

Table 2. Soil category according to their average wet unit weight

LIST OF FIGURES

- Fig. 1. Box diagram of undrained shear strength as a function of soil type. The undrained shear strength data include results of pocket penetrometer, unconfined compression test, and UU tests.
- Fig. 2. Correlation between undrained shear strength and liquidity index.
- Fig. 3. Correlation between undrained shear strength and liquid limit.
- Fig. 4. Correlation between undrained shear strength and preconsolidation stress.
- Fig. 5. Box diagram of undrained shear strength as a function of geological origin. The undrained shear strength data include results of pocket penetrometer, unconfined compression test, and UU tests.
- Fig. 6. Box diagram of S_u/σ_z' as a function of soil type. The undrained shear strength data include results of pocket penetrometer, unconfined compression test, and UU tests.
- Fig. 7. Correlation between S_u/σ_z' and liquidity index.
- Fig. 8. Correlation between S_u/σ_z' and liquid limit.
- Fig. 9. Correlation between S_u/σ_z' and plasticity index.
- Fig. 10. Correlation between S_u/σ_z' and OCR.
- Fig. 11. Correlation between S_u/σ_z' and preconsolidation stress.
- Fig. 12. Box diagram of S_u/σ_c' as a function of measurement method
- Fig. 13. Box diagram of S_u/σ_z' as a function of soil type. The undrained shear strength data include results of pocket penetrometer, unconfined compression test, and UU tests.
- Fig. 14. Box diagram of effective friction angle (ϕ') as a function of soil type.
- Fig. 15. Box diagram of cohesion (c') as a function of soil type.
- Fig. 16. Correlation between effective friction angle ϕ' and plasticity index
- Fig. 17. Correlation between $\sin\phi'$ and plasticity index
- Fig. 18. Correlation between c'/σ_z' and plasticity index
- Fig. 19. Box diagram of c'/σ_z' (only 41 pairs of c'/σ_z' and the corresponding PI in Fig. 18)
- Fig. 20. Box diagram of cohesion (c) as a function of geological origin.

Fig. 21. Box diagram of effective angle of friction (ϕ') as a function of geological origin.

Fig. 22. Box diagram of preconsolidation stress as a function of soil type.

Fig. 23. Box diagram of compression index (C_c) as a function of soil type.

Fig. 24. Correlation between compression index and swell index.

Fig. 25. Correlation between compression index and liquid limit.

Fig. 26. Correlation between compression index and in situ void ratio.

Fig. 27. Box diagram of preconsolidation stress as a function of geological origin.

Fig. 28. Box diagram of compression index as a function of geological origin.

Fig. 29. Box diagram of $C_c/(1+e)$ as a function of geological origin.

Fig. 30. Box diagram of OCR as a function of geological origin.

Fig. 31. Correlation between undrained shear strength and SPT-N.

Fig. 32. Correlation between undrained shear strength and SPT- N_{60} . The undrained shear strength data are measured by pocket penetrometer.

1. INTRODUCTION

The design of the Milwaukee Marquette Interchange project involved an extensive subsurface investigation for the structure and roadway foundations. The Milwaukee Transportation Partners (MTP) consultant team oversaw this work. The investigation involved soil borings, laboratory testing of various types of soil samples, and in-situ field-testing. Laboratory testing consisted of tests such as unconfined compression, consolidation, triaxial, moisture content, Atterberg limits, loss on ignition, compaction, gradation, pocket penetrometer, pH, resistivity, wet unit weights, California bearing ratio, etc. In-situ testing consisted of pressuremeter, dilatometer and piezometric cone penetration tests. This rather large volume of soil data offers a unique opportunity to compare the various laboratory and in-situ test results of these soil types.

This study investigates all of the generated soils data in an attempt to use the more 'routine' laboratory tests to determine geotechnical design parameters (such as ϕ -angle, cohesion, wet unit weight, unconfined compression, consolidation characteristics, etc.) that are typically obtained from more sophisticated laboratory tests or in-situ field tests. The test result data are analyzed to determine ranges of values, variations, trends, comparisons, etc. Since both routine and higher-level testing has been conducted, this comparison was made and correlations were developed that relate parameters for more sophisticated tests to those from simpler and more routine tests. Future design work in this area of the state could be based on more routine tests, while minimizing the need for more elaborate (and expensive) laboratory or in-situ tests. This is likely to lead to more economical subsurface investigations and greater confidence in soil properties

The Wisconsin Department of Transportation (WisDOT) has committed to a large improvement program of the freeway system in southeastern Wisconsin. Thus, the results of this study may enable reducing the design costs associated with the future projects in this area.

2. RESEARCH OBJECTIVE

The technical objective of this study is to review the generated soils data in the Milwaukee Marquette Interchange project in an attempt to correlate the more 'routine' laboratory tests to determine geotechnical design parameters (such as phi-angle, cohesion, wet unit weight, unconfined compression, consolidation characteristics, etc.) that are typically obtained from more sophisticated laboratory tests or in-situ field tests. The range of values, variations, trends and correlation will be explored in terms of different types of soils and/or geological origin and compared to published correlations whenever possible.

3. BACKGROUND

WisDOT has provided copies of all subsurface investigation information from the Marquette Interchange (MI) to the research team. This included boring logs and laboratory test results. Communications with WisDOT personnel indicated that most of the data are in electronic form, but some information is in paper format. The researchers reviewed all provided information and looked for trends, comparisons, ranges of values, etc. that can be used to correlate the different test methods to actual conditions. Engineering properties of glacial units from Southeastern Wisconsin have been compiled by Edil and Mickelson (1995) and provided an initial background to the geological origin and general characteristics of the soil units encountered at Marquette Interchange project. The portion of the data relating to structural properties (i.e., friction angle, cohesion and consolidation parameters) was

reviewed with respect to geological origin as determined from the stratigraphic position in the boring logs, soil descriptions, and index properties. The structural properties were then correlated with geological unit designation.

The focus has been to arrive at 'basic' soil field or laboratory tests that can be correlated to more sophisticated laboratory tests or in-situ tests. Use of such correlations would enable reducing the need for more expensive field and laboratory procedures on future projects in similar soil conditions. The findings and conclusions are expected to result in final recommendations on the suitability of using more basic laboratory or field tests to arrive at geotechnical design parameters that are typically found through more expensive laboratory tests or field investigative procedures for these particular soils. This report includes the analyses, findings, conclusions, and recommendations for appropriate use of the correlations.

There are prominent property correlations that have been published and found wide acceptance in the geotechnical community. These correlations, being empirical in essence, are, in principal, only applicable to the soils of the geological origin and/or of similar fundamental characteristics on which the correlation is based. Therefore, use of these correlations with confidence for local soils requires verification based on local data and identification of potential limitations. Such correlations can be found in most soil mechanics books (Mitchell 1996, Holtz and Kovacs 1983, Das 2006). Some of the correlations are also given in Design Manuals such as NAV FAC D7 (NAV FAC 1986). In a recent report, the Center for Geotechnical Practice and Research at Virginia Polytechnic Institute and State University, published shear strength correlations (Duncan 1989).

The correlations are given separately for cohesionless and cohesive soils in terms of index properties (e.g., gradation, Atterberg limits, density, soil type, etc.) and include the following:

- Friction angle for cohesionless soils in terms of index properties.
- Undrained shear strength and undrained shear strength ratio (i.e., undrained strength divided by overburden pressure) of cohesive soils.
- Effective friction angle and cohesion intercept of cohesive soils as related to specific till units and their geological history (Edil and Mickelson, 1995).

Compression/consolidation properties have also been correlated to index properties. These include:

- Compression index, which is correlated to various index properties (Azzouz et al. 1976).
- Swell index, which is related to compression index.
- Compression index, which is related to liquid limit (NAV FAC 1986).
- Preconsolidation stress as related to specific till units and their geological history (Edil and Mickelson, 1995).

A compilation of correlations between soil properties and in situ tests has been published in conjunction with the International Conference on In Situ Measurement of Soil Properties and Case Histories sponsored by the International Society for Soil Mechanics and Geotechnical Engineering (Rahardjo 2001). The various correlations include those for

- Shear strength (friction angle of cohesionless soils and undrained strength of cohesive soils) by SPT, pressuremeter, dilatometer and cone penetrometer tests.
- Consolidation characteristics.

These documents provide a background and starting point for evaluating potential correlations for the Marquette Interchange data.

This research effort is expected to produce a comprehensive examination of the potential of using lower cost field and laboratory tests to arrive at geotechnical design parameters similar to those obtained from more costly tests for soils common to southeastern Wisconsin. The study examines the correlation between the various test results. The variation in these values can be reviewed and criteria can be developed that delineate the appropriate use of parameters from the correlations for WisDOT projects in this area of the state. Documentation (data and information) will also be provided to assure that these correlations are appropriate.

4. MAIN APPROACH

4.1 Compilation of Data in Electronic Media

Most of the data were compiled in electronic media for easy manipulation and analysis and was transmitted as Microsoft Excel files. This database is included on 2 CDs attached to this report. The data received from WisDOT consisted of a master summary table (Master Lab Summary.xls) containing all test results (laboratory and in situ). The data was accompanied by four "Geotechnical Exploration Data" reports, a "Core Investigation" report, two "Cone Penetration Testing (CPT)" reports, a map of boring log locations, a geologic description of the site, and a file containing potential geotechnical research topics for the project. These files have been placed in the "Initial WisDOT Reports" folder and can be found in the attached CD labeled "Marquette – WisDOT Files".

The initial reports, however, contained only one third of the logs for the borings in the master summary table. Thirty three additional reports were received from WisDOT (Marquette-

WisDOT Files and Additional Reports CD) and the data was input in **Bold** in the master summary table (Master Lab Summary_Updated.xls). Even so, some boring logs could not be found. A list of missing boring logs can be found in the Appendix A. This master summary table contains all of data for data analysis, as shown in Table A1.

Additional boring logs were used for entering groundwater table (GWT) elevations and assigning Unified Soil Classification System (USCS) symbols to each data point in the master summary table spreadsheet. The GWT elevations were not available for all data points because some boring logs did not contain GWT data.

A spreadsheet was also created for compiling consolidated undrained (CU) triaxial test results (Marquette_CU Triaxial). The spreadsheet includes triaxial test results from WisDOT reports and from the laboratory tests conducted by the University of Wisconsin-Madison. Some data were reinterpreted, but not included in the master summary table. This file was created for summarizing and comparing all CU triaxial test results.

There are 3,763 samples in the boring logs. Table 4.1 and additional Table B.1 (in Appendix B) include the field measurement and laboratory measurement results. Table 4.1 summaries boring numbers and their sample interval depth, depth to center, elevation of sample, water table elevation, overburden stress, USCS soil classification from boring logs, soil type, standard penetration test (SPT) blow count, water content, wet unit weight, dry unit weight, loss of ignition, Atterberg limits (liquid limit, plastic limit, plasticity index, liquidity index), sieve analysis (P10, P40, P200, %silt, %clay), specific gravity, consolidation (void ratio, preconsolidation stress σ_c' , compression index C_c , swell index C_s , over-consolidation ratio OCR), unconfined compressive strength q_u from field pocket penetrometer and from laboratory unconfined compression test, unconsolidated-undrained triaxial test, consolidated-

undrained triaxial test (cohesion c , friction angle ϕ , effective cohesion c' , and effective friction angle ϕ'), hydraulic conductivity, max dry unit weight and optimum water content, pH, resistivity, CBR, sulfates and chlorides.

4.2 Identification of Potential Correlations

A systematic review of the literature was undertaken at the onset of the study to identify potential correlations, such as:

- Internal friction angle (ϕ') vs plasticity index (PI)
- S_u vs Liquidity Index (LI)
- S_u /overburden stress (S_u/σ_o') vs overconsolidation ratio (OCR)
- S_u vs water content

Most of the data was not paired in terms of structural and index properties, limiting the number of data points available for creating correlations. For example, this problem was encountered for creating a correlation between S_u/σ_o' and OCR. The wet unit weights for calculating overburden stresses were not available for all boring logs. Thus, USCS symbols were assigned to each data point (as obtained from the available boring logs) and the wet unit weights were plotted as a function of depth (wet unit weight vs depth). Soils containing similar wet unit weights were then divided into Type 1 (CL, CL-ML, HF, ML, ML-SM, SC-SP, SM, SM-ML-CL) and Type 2 (OH, OL, OL-CL, OL-ML, PT). Type 1 soils had an average wet unit weight of 137 ± 7 pcf (coefficient of variation of 5%), whereas Type 2 soils had an average wet unit weight of 105 ± 12 pcf (coefficient of variation of 11%) (Table 2). These wet unit weights are consistent with reported values for inorganic fine grained Wisconsin glacial soils, i.e., tills and lacustrine deposits are reported to have wet unit weights 130-138 pcf

(SEPRC 1989; Appendix E). Lower wet unit weight for organic soils is consistent with lower specific gravity of organic content. Effective overburden stresses were then calculated based on the aforementioned densities, available GWT elevations, and the depth of the data points. Preconsolidation stresses for calculating OCR were available in the master laboratory summary spreadsheet.

4.3 Statistical Analysis and Interpretation

In this phase a detailed analysis of the collected data to determine range of values, variations, trends, influencing factors and correlations with them, geological controls and other pertinent details were undertaken in so far as possible. Variations and ranges in the reported data, factors influencing such variations, trends based on geological origin, grain size distributions, Atterberg limits or other factors, correlations with index properties and geological origin, comparisons with typical assumed and published values, and other significant findings are included in the analysis.

Statistical methods were used to identify and develop reliable correlation equations. Analysis of variance (ANOVA) techniques were used to identify variables with statistically significant correlations. Based on the findings of the ANOVA, correlation equations were developed using regression procedures, such as stepwise multivariate regression. Non-linear regression techniques were also applied if needed. These techniques have been found to be very effective in developing reliable and easy-to-use correlation equations for geotechnical data. For example, Benson et al. (1994) used these techniques to develop an equation for predicting the hydraulic conductivity of clayey soils based on Atterberg limits, clay content, and gravel content. Similarly, Blotz et al. (1998) used these techniques to develop a rapid method to determine optimum water content and dry unit weight based on the liquid limit.

The analysis also addressed the suitability and accuracy of the correlation equations, and provided explicit criteria regarding suitable applications. Accuracy of the equations are explicitly defined so that engineers using the equations will understand the uncertainty associated with the estimated parameters and the limitations of the correlation equations when making design calculations.

An evaluation of existing empirical equations was also conducted. This evaluation includes an assessment of the suitability and accuracy of existing equations for soils in Wisconsin. Comparisons are also made between existing correlation equations and those determined using the aforementioned regression techniques.

5. RESULTS AND DISCUSSIONS

5.1 Geological Origin

The Menomonee River occupies a deep East-West valley under the city of Milwaukee and the Marquette Interchange is centered over the deepest part. Deposits in this valley consist of several till units, lake sediment, and stream sediment. The stratigraphy and depositional environments of this deep valley fill are described by a Need (1983). The interpretation of stratigraphic units was based on this stratigraphic framework. Stratigraphic units described in this report are defined in Mickelson et al. (1984).

There is a record of three ice advances into the Menomonee River Valley beneath Milwaukee, each of which deposited at least one till layer and commonly more than one. Because glacier ice advanced into the river valley from the Northeast, a lake formed in the valley each time the mouth of the river was dammed. After ice retreated back off this location and into the Lake Michigan basin a lake formed again in the valley. Thus the sequence

above bedrock consists of alternating till and lake sediment. Above this, and inset into these deposits, are alluvial deposits formed after the last ice retreated.

An early ice advance deposited Tiskilwa till, but this apparently is not in any of the borings. This was not reported by Need (1983) either. The next youngest unit is till of the New Berlin Member of the Holy Hill Formation. This unit is a sandy silty till with numerous cobbles and boulders. This unit was evidently not penetrated by any of the borings examined in this study, although it is present in the valley.

The next youngest unit is the Oak Creek Formation. This is typically a gray clayey (CL) sediment that may be till or lake sediment. In the borings the only way to distinguish is by the presence or absence of pebbles and its uniformity in the core. In some cases the Oak Creek till is interbedded with lake sediment and in this case it is very difficult to tell them apart. Commonly the lake sediment is somewhat siltier than the till and if the description was precise enough this could also be used to distinguish till from lake sediment. It also appears that the till is somewhat more consolidated than the lake sediment, but only locally. Three ice advances deposited Oak Creek till with interbedded lake sediment. Presumably at least some consolidation took place during each of these advances as well as the subsequent Ozaukee advance.

The youngest unit is the Ozaukee Member of the Kewaunee Formation. This also consists of clayey till and lake sediment. All of this classifies as a CL soil, so the only way to distinguish from the boring descriptions is based on the abundance of pebbles. The till of the Ozaukee Member can be distinguished from till of the Oak Creek Formation by its pink or purpleish hue. This is the uppermost till unit in the valley. The post glacial Menomonee and Milwaukee River's eroded away the till in most places in the valley. Alluvial deposits accumulated in the

valley as the level of Lake Michigan rose between 10,000 and 5500 years ago. Most of these deposits contain some traces organic materials.

5.2 Strength

5.2.1. Undrained Shear Strength (S_u)

Box plots are shown in Figure 1 of the distribution of undrained shear strength as a function of soil type. The centerline in the box corresponds to the mean (50th percentile), the outer edges of the box correspond to the 25th and 75th percentiles, and the whiskers (outermost liners) correspond to the 10th and 90th percentiles of the undrained shear strength. The undrained shear strength data are measured by pocket penetrometer (PP), unconfined compression strength test (UC) and unconsolidated-undrained (UU) triaxial tests. The difference among the undrained shear strength using the three measurements for each type of soil are shown in Appendix C (Figures. C1-C5).

Undrained shear strength of sandy silt, silty clay, and silty sand are very similar, including their mean and distributions. The mean undrained shear strength of clay is the highest (125 kPa) while the undrained shear strength of organic clay is the lowest (35 kPa). The box diagrams of undrained shear strength of measured methods (pocket penetrometer, unconfined compression test and UU tests) are shown in the Appendix C.

Correlation between undrained shear strength and liquidity index ($LI = w-PL/PI$) is shown in Figure 2. The best-fit nonlinear correlation ($R^2 = 0.58$) between undrained shear strength (S_u) and liquidity index (LI) can be expressed by:

$$S_u = \frac{144.9}{e^{1.72 \cdot LI}} \quad (1)$$

The dash lines in the Figure 2 indicate the correlation within $\pm 2\sigma$. All of paired data (S_u vs LI) from the unconfined compression test are in the range of $\pm 2\sigma$. Some of S_u data from the pocket penetrometer are outside of the $\pm 2\sigma$ range.

Correlation between undrained shear strength and liquid limit is shown in Figure 3. The best-fit nonlinear correlation ($R^2 = 0.38$) between undrained shear strength (S_u) and liquid limit (LL) can be expressed by:

$$S_u = \frac{191.4}{e^{0.03LL}} \quad (2)$$

Figure 4 shows correlation between undrained shear strength and preconsolidation stress. The best-fit nonlinear correlation ($R^2 = 0.43$) between undrained shear strength (S_u) and preconsolidation stress (σ_c') can be expressed by:

$$S_u = 0.31\sigma_c' - 10 \quad (3)$$

The question mark represents the undrained shear strength data that are excluded in the correlation development. There are not any correlations between measured undrained shear strength and effective normal stress, as shown in Appendix C (Figure 12).

Box plots are shown in Figure 5 of the distribution of undrained shear strength as a function of geological origin. The undrained shear strength data are measured by pocket penetrometer (PP), unconfined compression strength test (UC) and unconsolidated-

undrained (UU) triaxial tests. Undrained shear strength of Oak Creek till has the highest mean value (96.8 kPa). The mean undrained shear strength of Lacustrine soils (lake sediment) is 77.7 kPa while the undrained shear strength of Ozaukee till is 76.1 kPa (only one point). These strengths indicate that the glacial tills and lacustrine soils encountered are “stiff” soils.

As can be seen, the correlations of undrained strength with index properties or effective overburden stress by itself are not very strong. This is partly is a result of the fact that the most of the data are based on pocket penetrometer test but also it is a result of the fact that both composition (i.e., index properties) and stress history (i.e., density) separately control undrained strength. In the next section, a normalization of undrained strength with effective overburden stress and then correlation with index properties is considered.

5.2.2. Undrained Shear Strength over Effective Overburden Stress (S_u/σ_z')

Box plots are shown in Figure 6 of the distribution of S_u/σ_z' as a function of soil type. The S_u/σ_z' of clay and silty clay are similar, although there is broader distributed S_u/σ_z' of clay. The mean S_u/σ_z' of sandy silt and silty sand are comparable (~ 0.72). The mean S_u/σ_z' of organic clay is the lowest (0.26). These values are mostly higher than reported for normally consolidated soils, i.e., 0.23 ± 0.04 (Jamiolkowski et al. 1985). The implication is these soils are likely to be over consolidated to some degree except perhaps organic clay. The box diagrams of S_u/σ_z' from pocket penetrometer, unconfined compression test and UU tests are shown in the Appendix C (Figures C7-C11).

Correlation between S_u/σ_z' and liquidity index is shown in Figure 7. The best-fit nonlinear correlation ($R^2 = 0.32$) between S_u/σ_z' and LI can be expressed by:

$$\frac{S_u}{\sigma_z'} = \frac{0.5}{e^{1.1LI}} \quad (4)$$

Most of paired data (S_u/σ_z' vs LI) from the unconfined compression test are in the range of $\pm 2\sigma$. Some of S_u/σ_z' data from the pocket penetrometer are outside of the $\pm 2\sigma$ range. A similar relationship between S_u/σ_z' and LI has also been presented by Holtz and Kovacs (1981) and Mitchell and Soga (2005).

Correlation between S_u/σ_z' and liquid limit is shown in Figure 8. The best-fit nonlinear correlation ($R^2 = 0.12$) between S_u/σ_z' and LL can be expressed by (Mesri 1989):

$$\frac{S_u}{\sigma_z'} = 0.22 \quad (5)$$

Correlation between S_u/σ_z' and plasticity index is shown in Figure 9. The best-fit nonlinear correlation ($R^2 = 0.17$) between S_u/σ_z' and PI can be expressed by:

$$\frac{S_u}{\sigma_z'} = 0.11 + 0.01 \cdot PI \quad (6)$$

Most of paired data (S_u/σ_z' vs PI) from the unconfined compression test are in the range of $\pm 2\sigma$. Some of S_u/σ_z' data from the pocket penetrometer are outside of the $\pm 2\sigma$ range.

A linear relationship between S_u/σ_z' and PI has been presented by Mitchell and Soga (2005) based on Wroth and Houlsby (1985) as

$$\frac{S_u}{\sigma_z'} = 0.129 + 0.00435 \cdot PI \quad (7)$$

However, there are five relationship between S_u/σ_z' and PI that have been developed for “young”, “aged”, “special clays” (Holtz and Kovacs 1981). In this study, S_u/σ_z' and PI data supports the linear relationship between S_u/σ_z' and PI, as given by Eq. 6, which is reasonably close to Eq. 7 given by Wroth and Houlsby (1985)..

Figure 10 shows correlation between S_u/σ_z' and overconsolidation ratio. The best-fit nonlinear correlation ($R^2 = 0.67$) between S_u/σ_z' and OCR can be expressed by

$$\frac{S_u}{\sigma_z'} = 0.24 \cdot OCR^{1.1} \quad (8)$$

The question mark represents the S_u/σ_z' data that are excluded in the correlation development. A similar relationship between S_u/σ_z' and OCR has been reported in by Holtz and Kovacs (1981) and Mitchell and Soga (2005), although there is no correlation model developed. It is interesting to note that for OCR=1 (i.e., normally consolidated), Eq. 8 results in 0.24 which is very close to 0.23 ± 0.04 reported by Jamiolkowski et al. (1985) for normally consolidated soils. It is noted that some data points corresponds to OCR<1, i.e., underconsolidated. This is not likely and it is a consequence of the fact that effective

overburden stress was calculated for computing OCR based on estimated wet unit weights and groundwater table positions.

Correlation between S_u/σ_z' and preconsolidation stress σ_c' is shown in Figure 11. The best-fit nonlinear correlation ($R^2 = 0.11$) between S_u/σ_z' and σ_c' can be expressed by the Eq. 5 (Mesri 1989).

Box plots are shown in Figure 12 of the distribution of S_u/σ_c' (i.e., undrained strength normalized by preconsolidation stress) measured by pocket penetrometer (PP), unconfined compression strength test and UU triaxial tests. The mean S_u/σ_c' measured by unconfined compression strength test is 0.25, which is close to the 0.23 ± 0.04 reported by Jamiolkowski et al. (1985). The S_u/σ_c' measured by PP are much broad and have a higher mean (0.8) than unconfined compression test and UU triaxial test.

Box plots are shown in Figure 13 of the distribution of S_u/σ_z' as a function of geological origin. The S_u/σ_z' data are measured by PP, UC and UU triaxial tests. S_u/σ_z' of Lacustrine has the mean value (0.28), which is close to 0.22 reported by Mesri (1989) implying normal consolidation or slight overconsolidation. The S_u/σ_z' of Oak Creek till has the higher mean value (0.55) implying overconsolidation and broader distribution.

5.2.3. Drained Shear Strength (ϕ' and c')

Box plots are shown in Figure 14 of the distribution of effective friction angle (ϕ') as a function of soil type. The ϕ' of silty clay has a smaller mean (29°) but with a broader distribution than ϕ' of organic clay. Box plots are shown in Figure 15 of the distribution of effective cohesion

(c') as a function of soil type. The c' of silty clay has a smaller mean (19 kPa) but with a broader distribution than c' of organic clay.

Correlation between ϕ' and plasticity index is shown in Figure 16. The relationship between ϕ' and PI can be expressed by:

$$\phi' = 29^\circ \quad (9)$$

In other words, there is no discernible dependency of ϕ' on PI in this relatively narrow range of PI= 5 to 25. Correlation between $\sin\phi'$ and plasticity index is shown in Figure 17. A best-fit nonlinear correlation between $\sin\phi'$ and PI has been developed (Mitchell and Soga 2005) as:

$$\sin\phi' = -0.1 \cdot \ln(\text{PI}) + 0.8 \quad (10)$$

The measured effective friction angle in this study are scattered around the correlation described by Eq. 10.

Box plots are shown in Figure 18 of the distribution of ϕ' as a function of geological origin. ϕ' of Lacustrine soils has the lowest mean value (24°). The ϕ' of Oak Creek till has the mean value of 29° and a broader distribution than that of Lacustrine soils. These effective friction angles are consistent with the angles reported by SEWRPC (1989) for Oak Creek till ($27^\circ - 31^\circ$) and fine-grained (clay and silt) lacustrine soils ($22^\circ - 27^\circ$).

There are no known correlations for c' other soil parameters. c' is a result of overconsolidation or stress history. c' is considered zero for normally consolidated clays and increases with increasing overconsolidation. There were no paired c' and OCR data to explore a relationship. c' is normalized with effective overburden stress. In this study, c'/σ_z' and PI data indicate that c'/σ_z' has a mean value of 0.2 but in no case is more than 1 as shown in Fig. 19. It also does not show any trends with PI. Box plots are shown in Fig. 20 of the distribution of c'/σ_z' measured by CU triaxial tests for all soils tested. The mean c'/σ_z' in this study is 0.2.

Box plots are shown in Figure 21 of the distribution of c' as a function of geological origin. c' of Lacustrine soils has the highest mean value (23 kPa). The c' of Oak Creek till has the mean value of 17.6 kPa and a broader distribution than that of Lacustrine soils. These effective cohesions follow consistent trend with the values reported by SEWRPC (1989) for Oak Creek till (5 kPa) and fine-grained (clay and silt) lacustrine soils (21 kPa) in that lacustrine soils exhibit higher effective cohesion compared to Oak Creek till.

5.3 Compression

Box plots are shown in Figure 22 of the distribution of preconsolidation stress (σ_c') as a function of soil type. The σ_c' of silty clay has a smaller mean (246 kPa) but with a broader distribution than σ_c' of sandy silt. Box plots are shown in Figure 23 of the distribution of compression index (C_c) as a function of soil type. The C_c of silty clay has a similar mean (0.08) but with a broader distribution than C_c of sandy silt.

Correlation between compression index (C_c) and swell index (C_s) is shown in Figure 24. The swell index is appreciably smaller in magnitude than the compression index. For most fine-

grained soils, it is reported that $C_s \approx (0.1 \text{ to } 0.2) C_c$ (Das 2006). In this study, most of the data fall between these limits, but some of data are out of range.

Correlation between C_c and liquid limit is shown in Figure 25. A best-fit nonlinear correlation between C_c and LL has been developed by Skempton (1944) as:

$$C_c = 0.009(LL - 10) \quad (11)$$

The measured C_c in this study are scattered around the correlation described by Eq. 11.

Correlation between C_c and in situ void ratio is shown in Figure 26. A best-fit nonlinear correlation between C_c and e_o has been developed (Hough 1957) as:

$$C_c = 0.3(e_o - 0.27) \quad (12)$$

The measured C_c in this study are reasonably consistent with the correlation described by Eq. 12.

Box plots are shown in Figure 27 of the distribution of σ_c' as a function of geological origin. σ_c' of Lacustrine soils has the highest mean value (270 kPa). The σ_c' of Oak creek till has the mean value of 236 kPa and a broader distribution than that of Lacustrine soils.

Box plots are shown in Figure 28 of the distribution of C_c as a function of geological origin. C_c of Lacustrine soils has the lowest mean value (0.07). The C_c of Oak Creek till has a mean value of 0.09 and a broader distribution than that of Lacustrine soils. These mean C_c

are very close perhaps reflecting the fact that till and lacustrine soils are derived from the similar sources and have comparable composition.

Box plots are shown in Figure 29 of the distribution of compressibility, $C_c/(1+e)$, as a function of geological origin. $C_c/(1+e)$ of Lacustrine soils has the lowest mean value (0.05). The $C_c/(1+e)$ of Oak Creek till has the mean value of 0.06 and a broader distribution than that of Lacustrine soils.

Box plots are shown in Figure 30 of the distribution of OCR as a function of geological origin. OCR of Lacustrine soils has the lowest mean value (0.08). The OCR of Oak creek till has the mean value of 1 and a broader distribution than that of Lacustrine soils. It is interesting to note that majority of OCR values are less than 1 (i.e., normally consolidated conditions). This is not likely to be correct. Nevertheless, Oak Creek till seems to have a slightly higher overconsolidation compared to Lacustrine soils which is a reasonable to expect. It should be pointed out that it is well known in Wisconsin that MOST glacial tills give OCR near 1 implying that they are normally consolidated following the standard procedures for calculating OCR (Edil and Mickelson, 1992) although they were subjected to ice loads. The reason for this is still not fully understood although Edil and Mickelson (1992) attribute it to groundwater fluctuations in geologic times.

5.4 Field Test

Correlation between undrained shear strength S_u and SPT N value as a function of soil type is shown in Figure 31. The distribution ranges of three soil types are separated. A similar correlation between undrained shear strength S_u and SPT N value can be found in NAV FAC (1986).

The measured SPN penetration number N was converted to standard penetration number N_{60} , with the following equation:

$$N_{60} = \frac{N \cdot \eta_H \cdot \eta_B \cdot \eta_S \cdot \eta_R}{60} \quad (13)$$

where the η_H is hammer efficiency (%), η_B is correction for borehole diameter, η_S is sampler correction, and η_R is correction for rod length. In this study, the η_H is 60%, η_S , η_B , and η_R are 1.0.

Correlation between undrained shear strength S_u and N_{60} is shown in Figure 32. A nonlinear correlation between S_u and N_{60} has been developed (Hara et al. 1971):

$$S_u = 29 \cdot N_{60}^{0.72} \quad (14)$$

The measured S_u and N_{60} in this study are scattered around the correlation described by Eq. 14.

6. CONCLUSIONS

A comparison of basic laboratory test results with more sophisticated laboratory and in situ tests methods on soils in Southeastern Wisconsin has been described in this report. The generated soils data in the Milwaukee Marquette Interchange project has been used in an attempt to correlate the more 'routine' laboratory tests to determine geotechnical design parameters (such as phi-angle, cohesion, unconfined compression, consolidation

characteristics, etc.) that are typically obtained from more sophisticated laboratory tests or in-situ field tests. The range of values, variations, trends and correlation were explored in terms of different types of soils and/or geological origin.

There were 3,763 boring logs samples and each boring logs included 54 types of data. Correlations were identified among undrained shear strength, effective friction angle, effective cohesion, consolidation parameters, soil type, Atterberg limits, effective overburden stress, and geological origin. Statistical analysis and interpretation were used to develop a detailed analysis of the collected data to determine range of values, variations, trends, influencing factors and correlations with them. ANOVA and non-linear regression techniques were applied to identify and develop reliable correlation equations.

Inorganic soils have an average wet unit weight of 137 ± 7 pcf, whereas organic soils 105 ± 12 pcf with small coefficient of variation. Undrained shear strength, measured by pocket penetrometer, unconfined compression strength tests and unconsolidated-undrained triaxial tests, is similar for sandy silt, silty clay and silty sand with a mean of 108 kPa. The undrained shear strength of Oak Creek till is higher than that of Lacustrine soils and Ozaukee till but all three soils classify as “stiff” soils. Organic soils have markedly lower undrained strength than these soils and classify as “medium stiff”. Regression analysis found that the undrained shear strength exponentially decreases with liquidity index and liquid limit with a reasonably stronger correlation with liquidity index. There are not any apparent correlations between measured undrained shear strength and effective overburden stress. This may be partly due to the fact some of the effective burden stresses were calculated in this study and were not reported in the original data.

Box plots of normalized undrained strength (S_u/σ_z') from unconfined compression tests for Lacustrine soil have a mean of 0.27-0.28, which is close to the reported 0.23 ± 0.04 in the literature. Mean S_u/σ_z' was higher for Oak Creek till (0.55) implying some over consolidation. Regression analysis found that S_u/σ_z' exponentially decreases with liquidity index and S_u/σ_z' is constant over liquid limit and preconsolidation stress σ_c' ($S_u/\sigma_z' = 0.22$). Using the best-fit nonlinear correlation, the S_u/σ_z' can be expressed by OCR with a power function. The relationship among S_u/σ_z' and these index properties are close to the published correlations in the literature. Box plots of S_u/σ_z' measured by unconfined compression tests has a mean of 0.22, which is also very close to reported values in the literature. The data of S_u/σ_z' and plasticity index also support the published linear relationship for these parameters.

Regression analysis found that effective angle of friction, ϕ' is constant over plasticity index ($\phi' = 29^\circ$) for the narrow range of plasticity indices measured (5-25). The data of $\sin\phi'$ and plasticity index are distributed around the published linear relationship for these parameters. Lacustrine soils have a higher effective cohesion, c' (mean 23 kPa) whereas Oak Creek till has lower effective cohesion (mean 17.6 kPa).

Compression index (C_c) and liquid limit are consistent with the published linear relationship for these parameters. Similarly, C_c and in situ void ratio correlation conforms with the published linear relationship between C_c and in situ void ratio. Correlation between compression index (C_c) and swell index (C_s) is found that most of data in this study are in the range of $C_s \approx 0.2$ to $0.1 C_c$, which is typical relationship between C_c and C_s .

Undrained shear strength (S_u) and standard penetration test blow count (SPT N) values can be grouped as a function of soil type. The distribution ranges of three soils types in this study

are similar to the published relationship between S_u and SPT N. The data of S_u and corrected SPT N for hammer efficiency (N_{60}) in this study are scattered around the published power relationship between S_u and N_{60} in the literature.

Correlations relating to effective strength parameters and compressibility are quite strong and can be used. Undrained strength is highly scattered partly because of the test method (i.e., pocket penetrometer); however, undrained strength normalized with effective overburden stress can be used with greater confidence.

7. RECOMMENDATIONS

Based on a consideration of the correlations investigated, their quality, and broad engineering background and judgement, the following recommendations are made.

Wet Unit Weights

Recommended Wet Unit Weights

	Inorganic Soils	Organic Soils
USCS Soil Type	CL, CL-ML, HF, ML, ML-SM, SC-SP, SM, SM-ML-CL	OH, OL, OL-CL, OL-ML, PT
Wet Unit Weight (pcf)	137 ± 7	105 ± 12

Undrained Strength

Recommended Undrained Shear Strength as a Function of Soil Type

USCS Soil Type		Undrained Shear Strength (kPa)	S_u/σ'_z
Inorganic Soils* $S_u = \frac{144.9}{e^{1.72 \cdot LI}}$	CL	125 ± 64	$\frac{S_u}{\sigma'_z} = 0.24 \cdot OCR^{1.1}$
	CL-ML	116 ± 64	
	ML	103 ± 64	
	SM	106 ± 64	
Organic Soils**	OL	35 ± 26	0.26

Recommended Undrained Shear Strength as a Function of Geological Origin

Geological Origin	Undrained Shear Strength (kPa)	OCR	S_u/σ'_z
Glacial Till (Oak Creek)*	97 ± 50	2	0.55
Lacustrine Deposits	78 ± 50	1	0.22

Drained Strength Parameters

Recommended Drained Strength Parameters as a Function of Soil Type

Soil Type	Effective Friction Angle (ϕ') (degrees)	Effective Cohesion Intercept, c' (kPa)	c'/σ'_z
Silty Clay	29 ± 8	0 to 19	0.2 (0 to 0.4)
Organic Soils	31 ± 2	27 ± 10	

Recommended Drained Strength Parameters as a Function of Soil Type

Geological Origin	Effective Friction Angle (ϕ') (degrees)	Effective Cohesion Intercept, c' (kPa)	c'/σ'_z
Oak Creek Till	29 ± 8	0 to 18	0.2 (0 to 0.4)
Lacustrine	24 ± 5	23 ± 13	
Fill	31 ± 7	0 to 19	

Compression Parameters

Recommended Compression Parameters

Compression Index, C_c	0.08 ± 0.05 or $C_c = 0.3(e_o - 0.27)$
Compressibility, $C_c/(1+e_o)$	0.06
Swell Index, C_s	1/10 C_c to 1/5 C_c
Preconsolidation Stress, σ'_c (kPa)	246 ± 147
OCR	1 to 2

8. REFERENCES

- Azzouz, A. S., Krizek, R. J. and Corotis, R. B. (1976). Regression Analysis of Soil Compressibility. *Soils and Foundations*, Vol. 16, No.2, 19-29.
- Benson, C. and Trast, J. (1995), Hydraulic Conductivity of Thirteen Compacted Clays, *Clays and Clay Minerals*, 43(6), 669-681.
- Benson, C., Zhai, H., and Wang, X. (1994), Estimating the Hydraulic Conductivity of Compacted Clay Liners, *J. of Geotech. Eng.*, ASCE, 120(2), 366-387.
- Blotz, L., Benson, C., and Boutwell, G. (1998), Estimating Optimum Water Content and Maximum Dry Unit Weight for Compacted Clays, *J. of Geotech. and Geoenvironmental Eng.*, ASCE, 124(9), 907-912.
- Das, B. M. (2006). Principles of Geotechnical Engineering, 6th Edition, Thomson.
- Duncan, M. J., (1989). Shear Strength Correlations, Practice Report Series, Center for Geotechnical Practice and Research, Virginia Polytechnic Institute and State University.
- Edil, T. B., Mickelson, D. M. and Acomb, L. J., (1977). Relationship of Geotechnical Properties to Glacial Stratigraphic Units Along Wisconsin's Lake Michigan Shoreline, *Proceedings of the 30th Canadian Geotechnical Conference*, Saskatoon, Saskatchewan, Session II, 36-54.
- Edil, T. B., R. J. Krizek, and J. S. Zelasko (1975), Effect of Grain Characteristics on Packing of Quartziferous Sands, *Proceedings of the Istanbul Conference on Soil Mechanics and Foundation Engineering*, Istanbul, Turkey, Vol. I, 46-54.
- Edil T.B. and Mickelson, D. M. (1995). Overconsolidated Glacial Till in Eastern Wisconsin, *Transportation Research Record*, No. 1479, Washington, D.C., 99-106.
- Hara, A., Ohata, T., and Niwa, M. (1971). Shear Modulus and Shear Strength of Cohesive Soils, *Soils and Foundations*, Vol. 14, No. 3, 1-12.
- Holtz, R. D. and Kovacs, W. D. (1981). An Introduction to Geotechnical Engineering, Prentice Hall, N.J.
- Jamiolkowski, M., Ladd, C.C., Germaine, J.T. and Lancellotta, R. (1985). New Developments in Field and Laboratory Testing of Soils. *Proceedings, XIth International Conference on Soil Mechanics and Foundation Engineering*, San Francisco, Vol. 1, 57-153.
- Mesri, G. (1989). A Re-evaluation of $s_{u(mob)} \approx 0.22\sigma_p$ Using Laboratory Shear Tests. *Canadian Geotechnical Journal*, Vol. 26, No. 1, 162-164.
- Mickelson, D. M., Acomb, L. J. and Edil, T. B., (1979). The Origin of Preconsolidated and Normally Consolidated Tills in Eastern Wisconsin, U.S.A., *Moraines and Varves* (Proceedings of the International Union for Quaternary Research Symposium, Zurich, Switzerland), A. A. Balkema, Rotterdam, 179-187.

- Mickelson, D.M., Clayton, L., Baker, R.W., Mode, W.N., and Schneider, A.F., (1984). *Pleistocene Stratigraphic Units of Wisconsin*. Wisconsin Geological and Natural History Survey, Miscellaneous Paper, 84-1, 199.
- Milwaukee Transportation Partners (2004). Geotechnical Exploration Data Report (Volume 1-4): Marquette Interchange Project at City of Milwaukee, Wisconsin for Wisconsin Department of Transportation.
- Mesri, G. (1973). Coefficient of Secondary Compression. *Journal of Soil Mechanics and Foundations Division*, Vol. 99, No. SM1, 123-137.
- Mesri, G. (1989). A Re-evaluation of $s_{u(mob)} \approx 0.22\sigma_p$ Using Laboratory Shear Tests. *Canadian Geotechnical Journal*, Vol. 26, No. 1, 162-164.
- Mitchell, J.K. and Soga, K. (2005), Fundamentals of Soil Behavior, 3rd Edition, Wiley, N.Y.
- NAV FAC (1986). Soil Mechanics, Naval Facilities Engineering Command, Design Manual DM 7.01, VA
- Need, E.A., (1983). Quaternary stratigraphy of the lower Milwaukee and Menomonee River valleys: In Mickelson, D.M. and Clayton, Lee (Eds.), *Late Pleistocene history of southeastern Wisconsin*. Wisconsin Geological and Natural History Survey, Geoscience Wisconsin v. 7, 111.
- Rahardjo, P. (2001). Correlations between Soil Properties and In Situ Tests. Supplementary Report, International Conference on In Situ Measurement of Soil Properties and Case Histories, International Society for Soil Mechanics and Geotechnical Engineering, Bali, Indonesia.
- Skempton, A. W. (1944). Notes on the Compressibility of Clays, *Quarterly Journal of the Geological Society of London*. Vol. 100, 119-135.
- Skempton, A. W. (1957). Discussion: The Planning and Design of New Hong Kong Airport, *Proceedings*, Institute of Civil Engineers, London, Vol. 7, 305-307.
- SEWRPC (1989). A Lake Michigan Shoreline Erosion Management Plan for Milwaukee County, Wisconsin. Southeastern Wisconsin Regional Planning Commission, Community Assistance Planning Report No. 163.
- Whited, G. C. and Edil, T. B. (1986). Influence of Bore Hole Stabilization Techniques on Standard Penetration Test Results, *Geotechnical Testing Journal*, American Society for Testing and Materials, Vol. 9, No. 4, 180-188.
- Wroth, C. P. and Houlsby, G. T. (1985). Soil Mechanics-Property Characterization and Analysis Procedures, *Proceedings of the 11th International Conference on Soil Mechanics and Foundation Engineering*, San Francisco, Vol. 1, 1-55.
- Zelasko, J., Krizek, R.J. and Edil, T.B. (1975). Shear Behavior of Sands as a Function of Grain Characteristics, *Proceedings of the Istanbul Conference on Soil Mechanics and Foundation Engineering*, Istanbul, Turkey, Vol. I, 55-64.

TABLES

Table 2. Soil category according to their average wet unit weight

	Type 1 Soil	Type 2 Soil
Soil Type	CL, CL-ML, HF, ML, ML-SM, SC-SP, SM, SM-ML-CL	OH, OL, OL-CL, OL-ML, PT
Wet Unit Weight	137 ± 7 pcf (coefficient of variation of 5%)	105 ± 12 pcf (coefficient of variation of 11%)

FIGURES

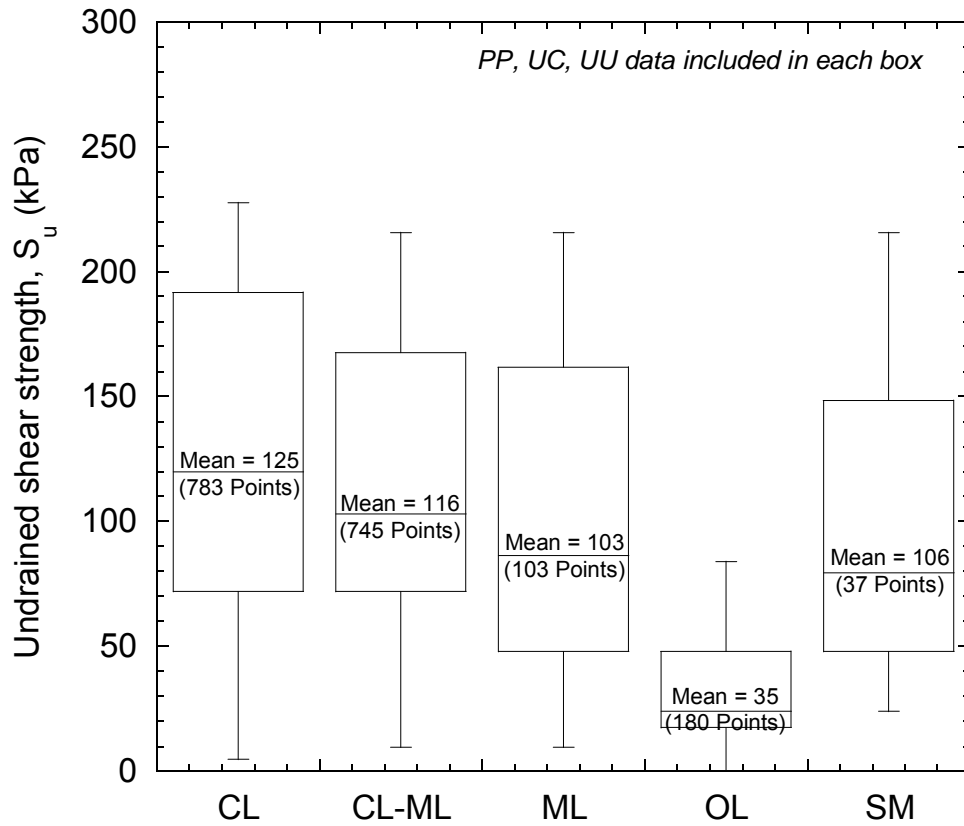


Fig. 1. Box diagram of undrained shear strength as a function of soil type. The undrained shear strength data include results of pocket penetrometer, unconfined compression test, and UU tests.

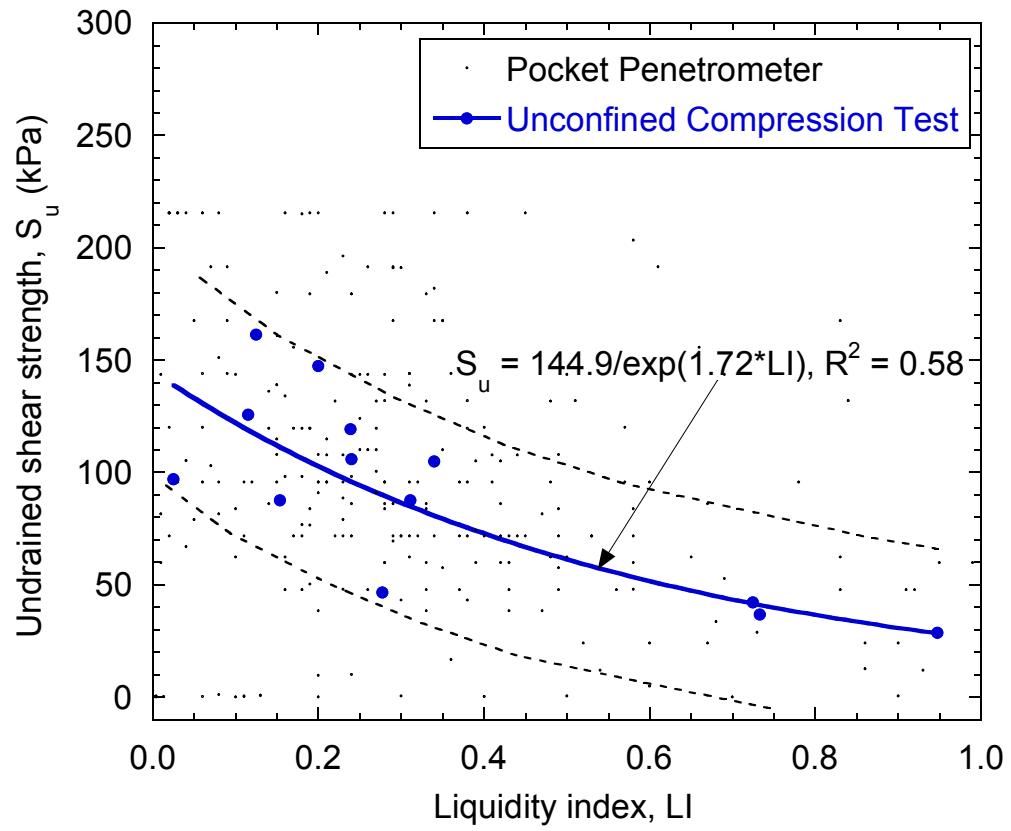


Fig. 2. Correlation between undrained shear strength and liquidity index.

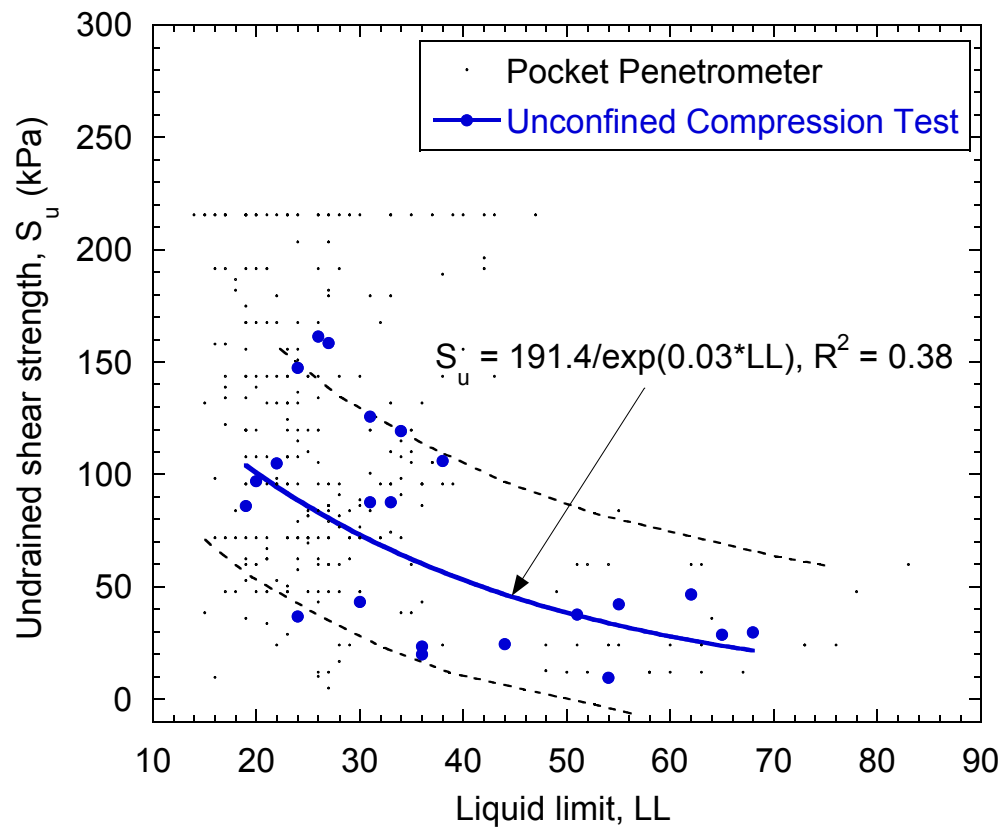


Fig. 3. Correlation between undrained shear strength and liquid limit.

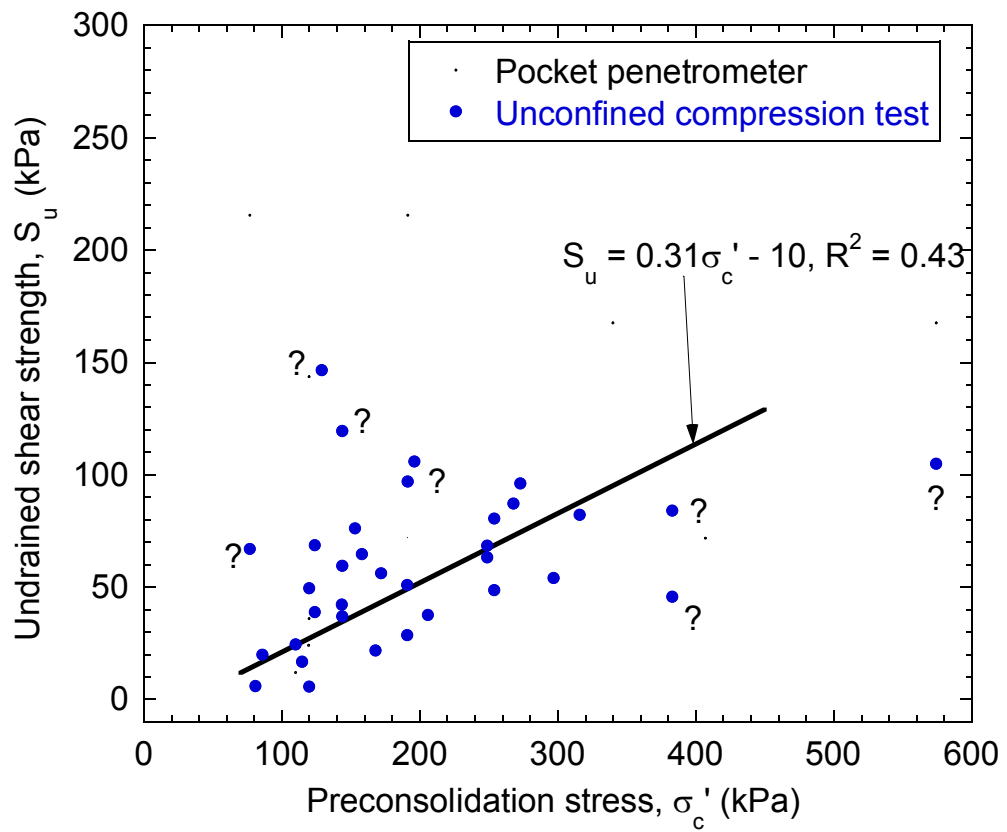


Fig. 4. Correlation between undrained shear strength and preconsolidation stress.

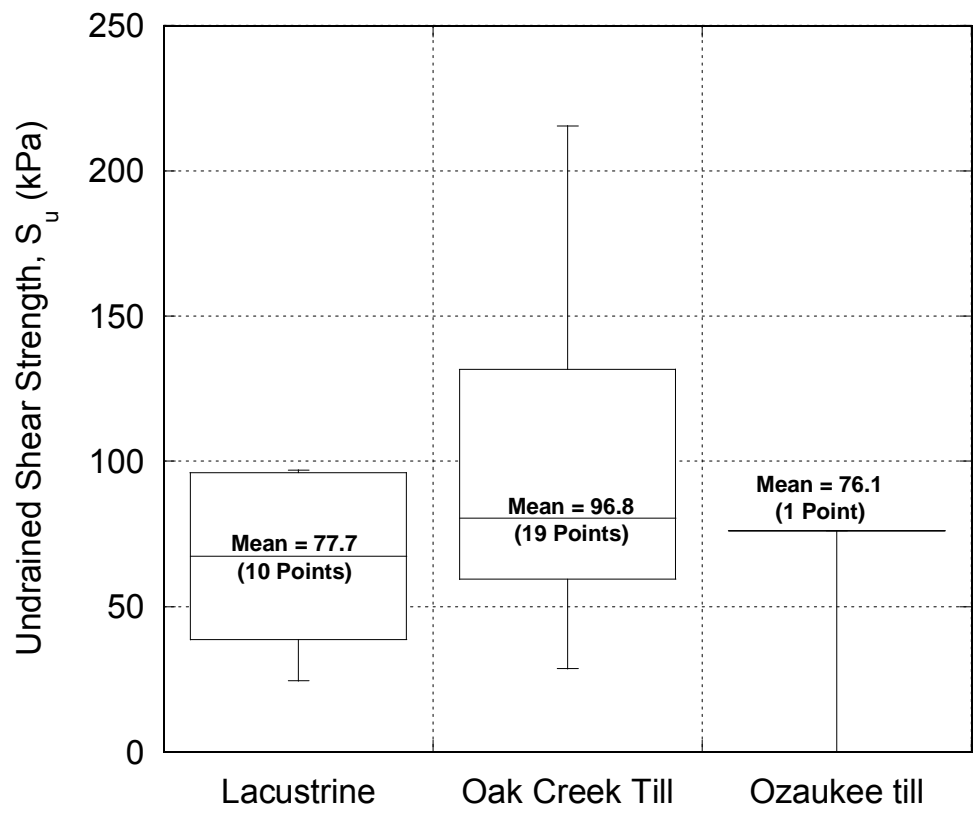


Fig. 5. Box diagram of undrained shear strength as a function of geological origin. The undrained shear strength data include results of pocket penetrometer, unconfined compression test, and UU tests.

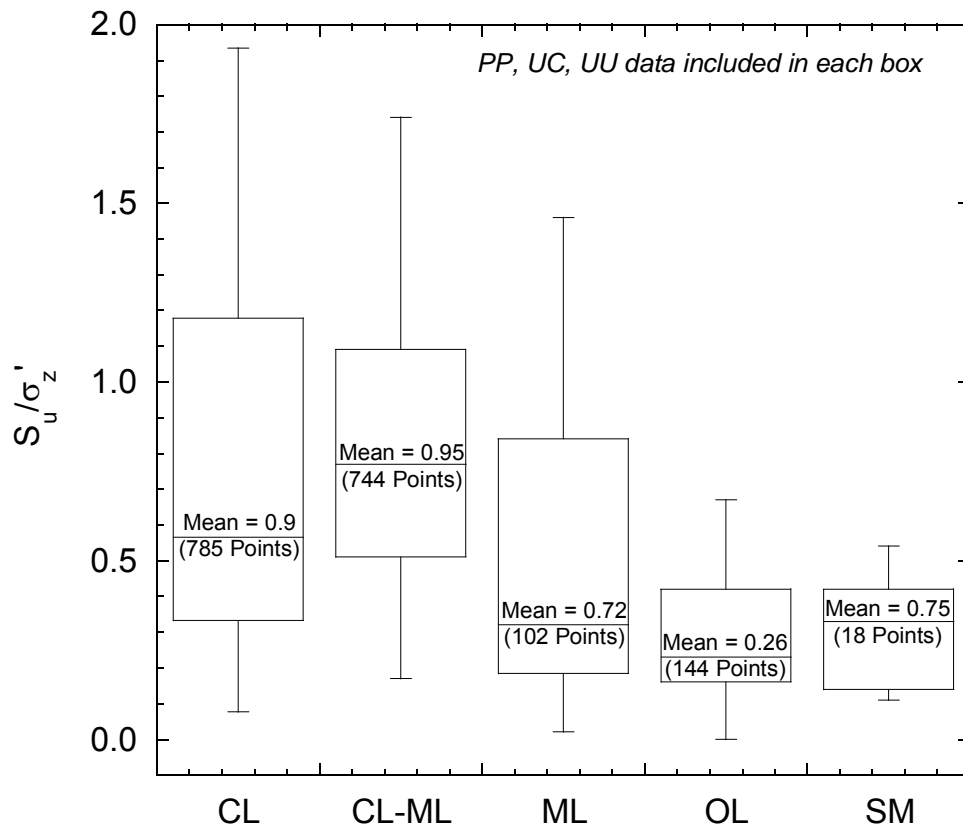


Fig. 6. Box diagram of S_u/σ'_z as a function of soil type. The undrained shear strength data include results of pocket penetrometer, unconfined compression test, and UU tests.

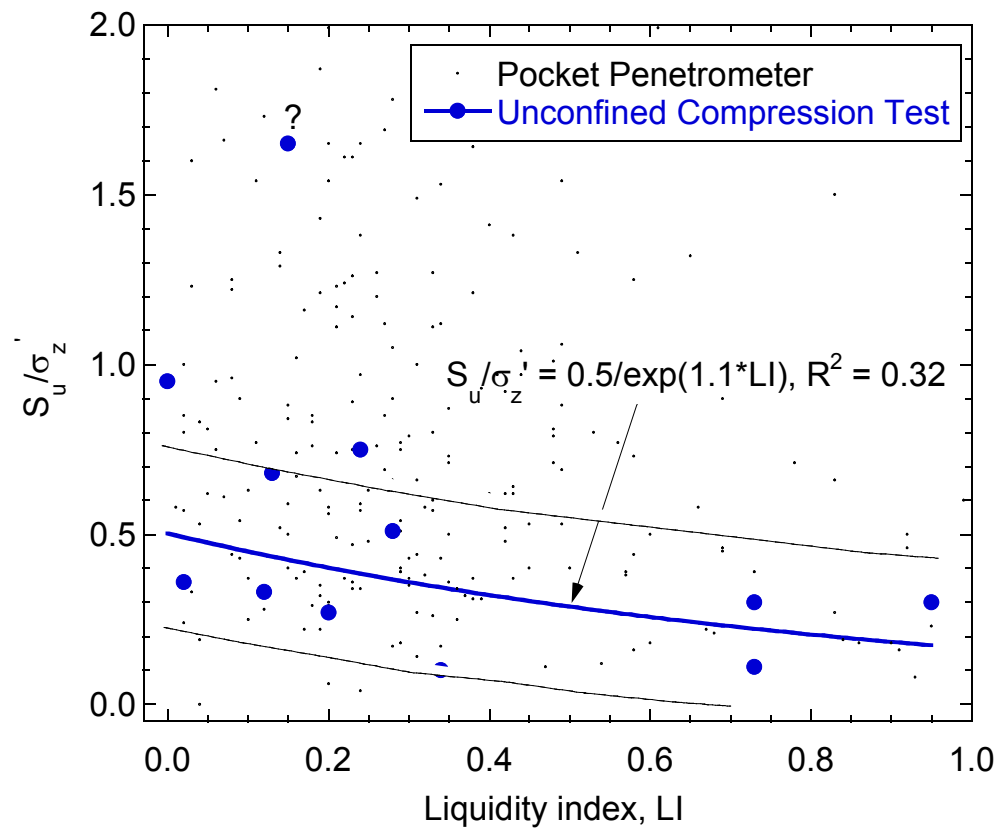


Fig. 7. Correlation between S_u/σ'_z and liquidity index.

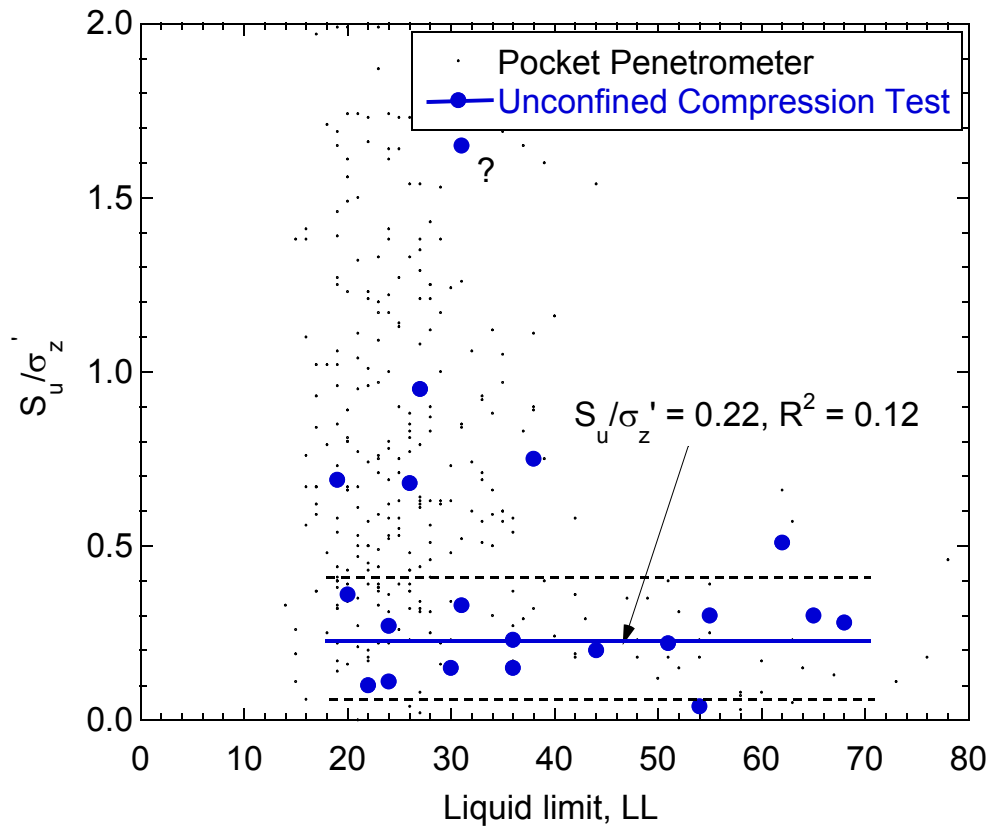


Fig. 8. Correlation between S_u/σ'_z and liquid limit.

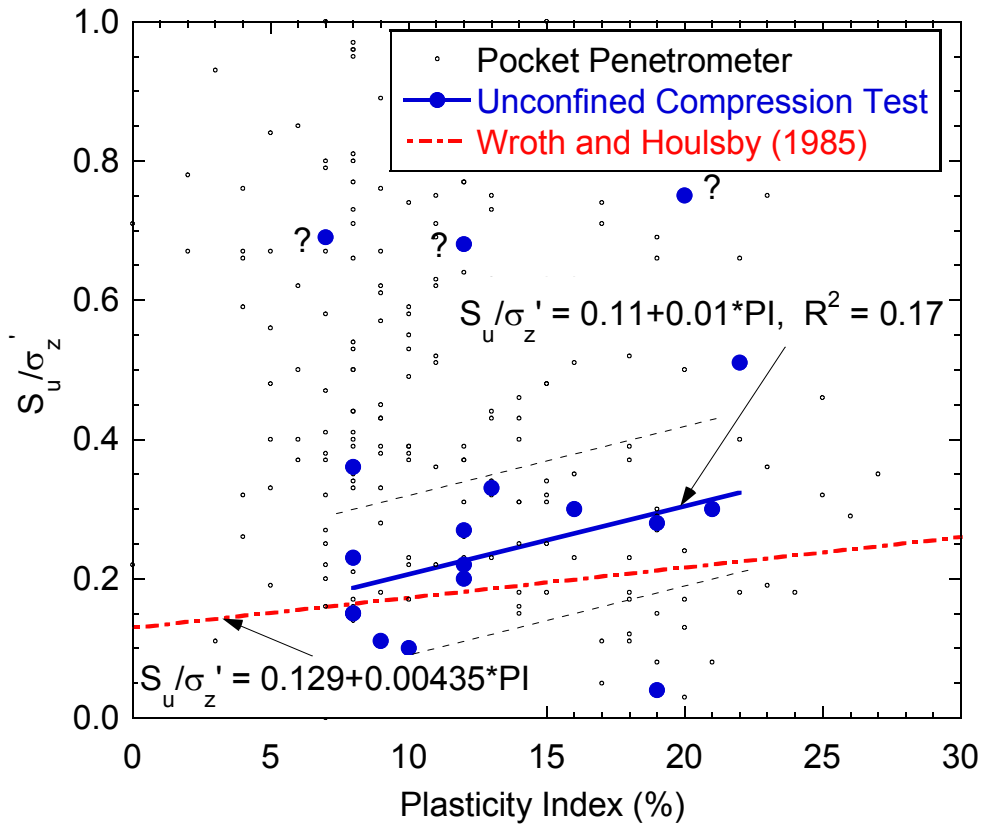


Fig. 9. Correlation between S_u/σ'_z and plasticity index.

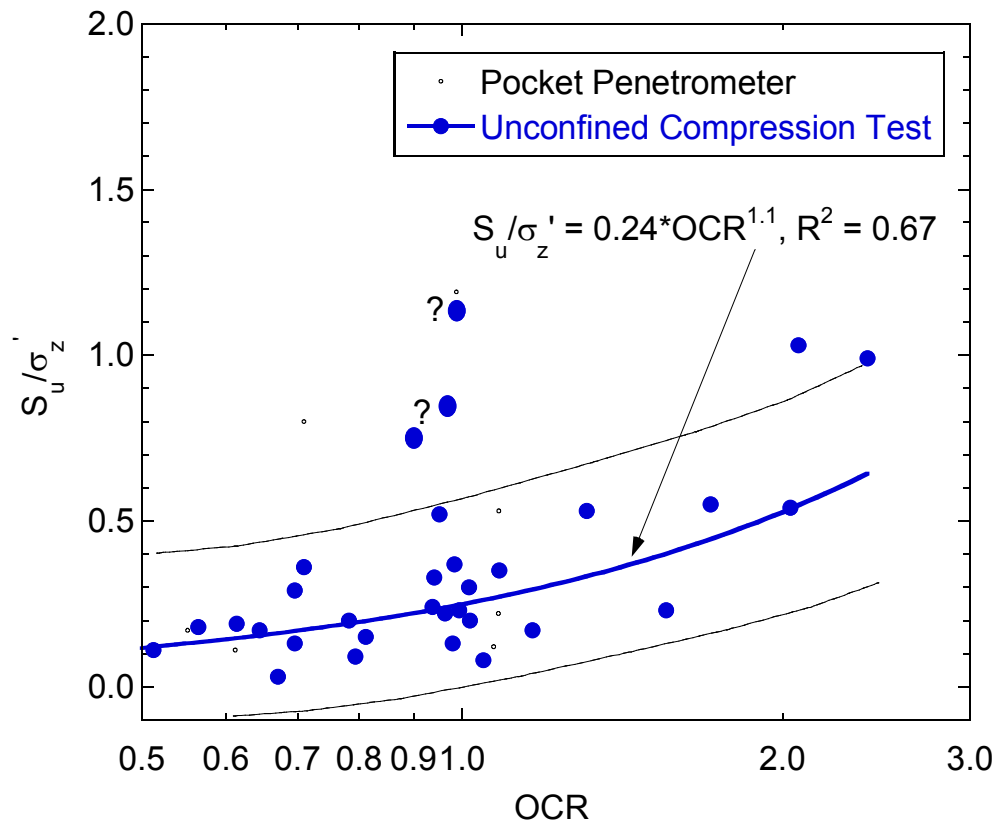


Fig. 10. Correlation between S_u/σ'_z and OCR.

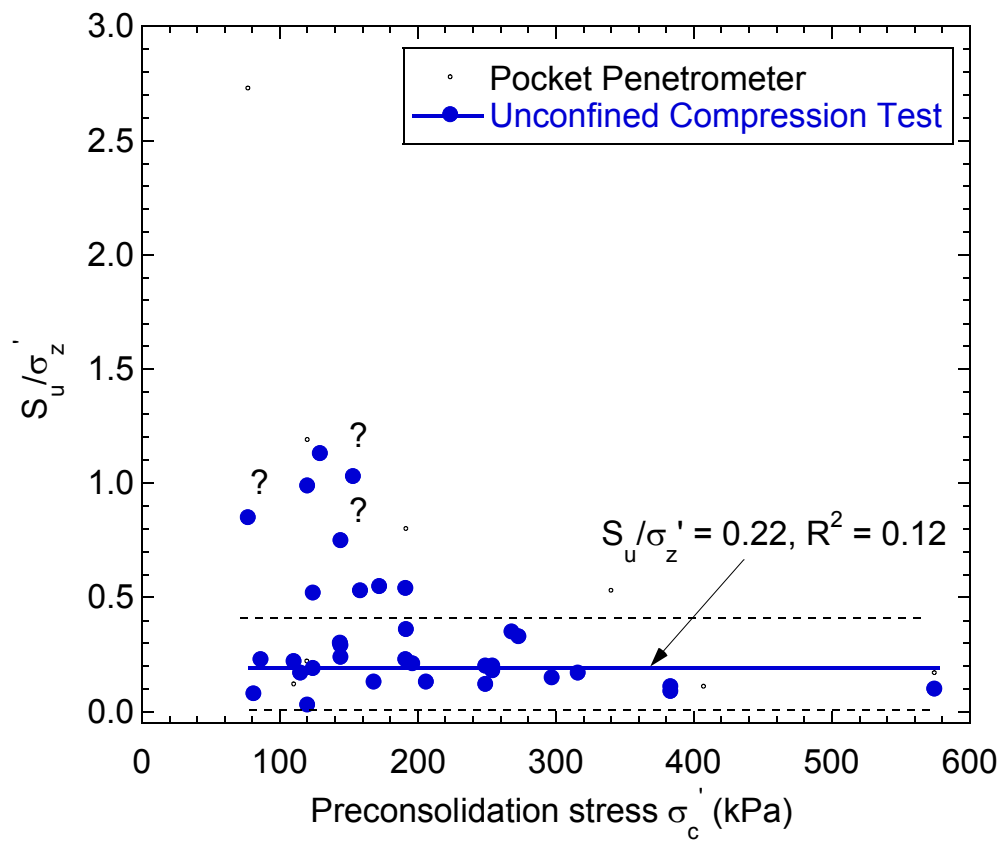


Fig. 11. Correlation between S_u/σ'_z and preconsolidation stress.

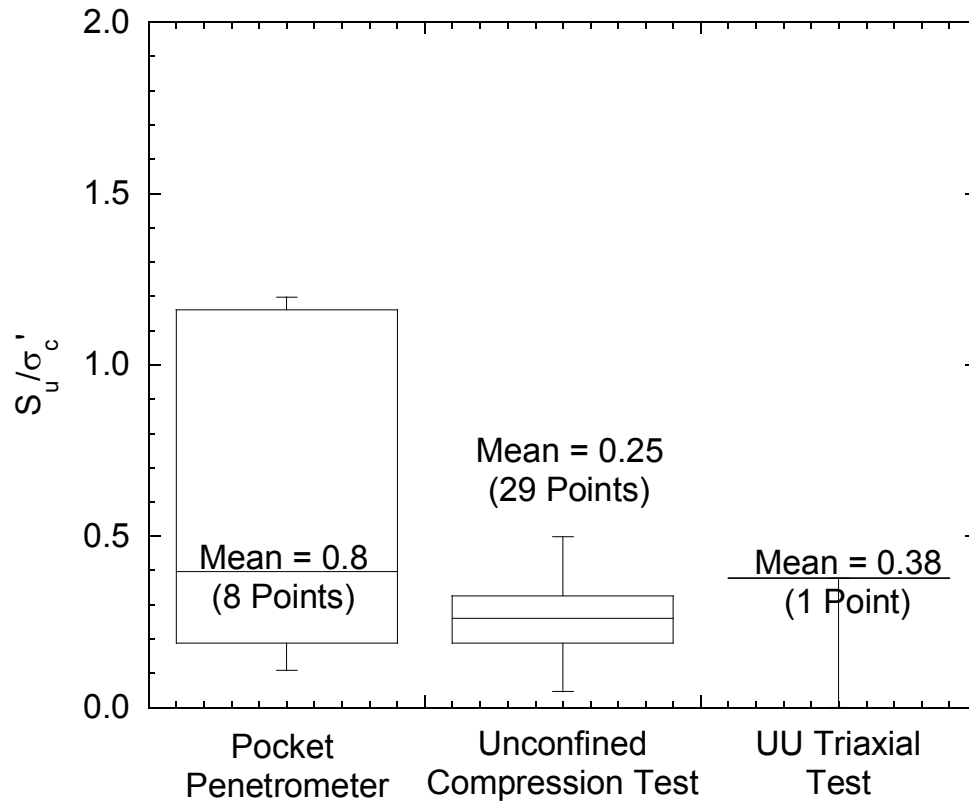


Fig. 12. Box diagram of S_u/σ'_c as a function of measurement method

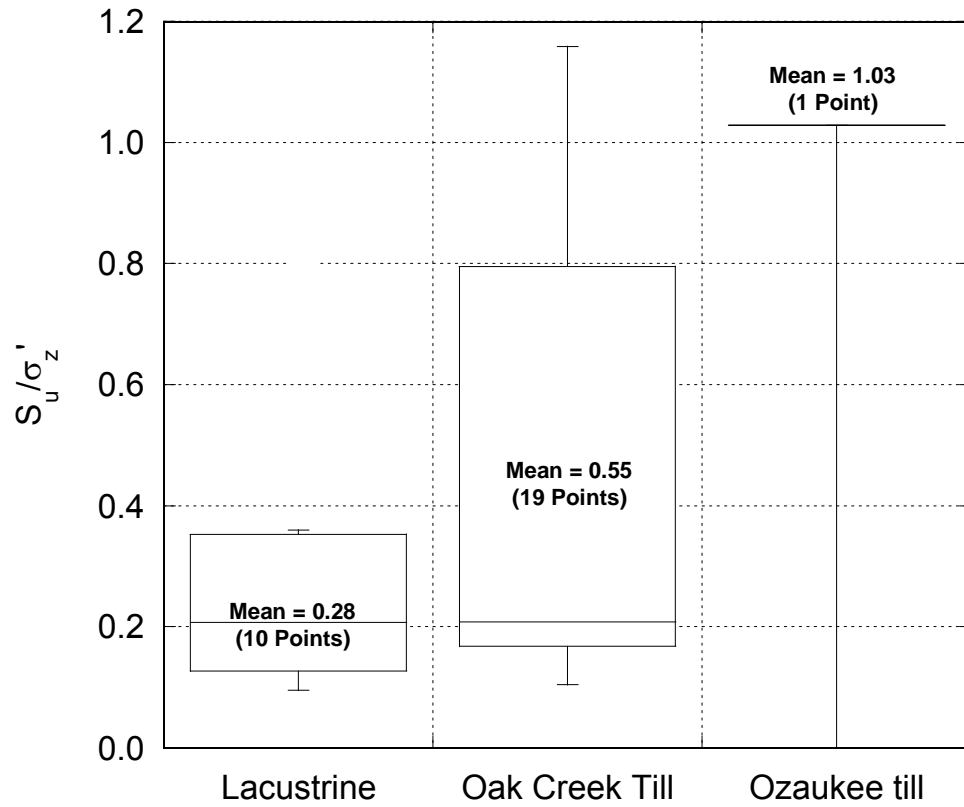


Fig. 13. Box diagram of S_u/σ'_z as a function of soil type. The undrained shear strength data include results of pocket penetrometer, unconfined compression test, and UU tests.

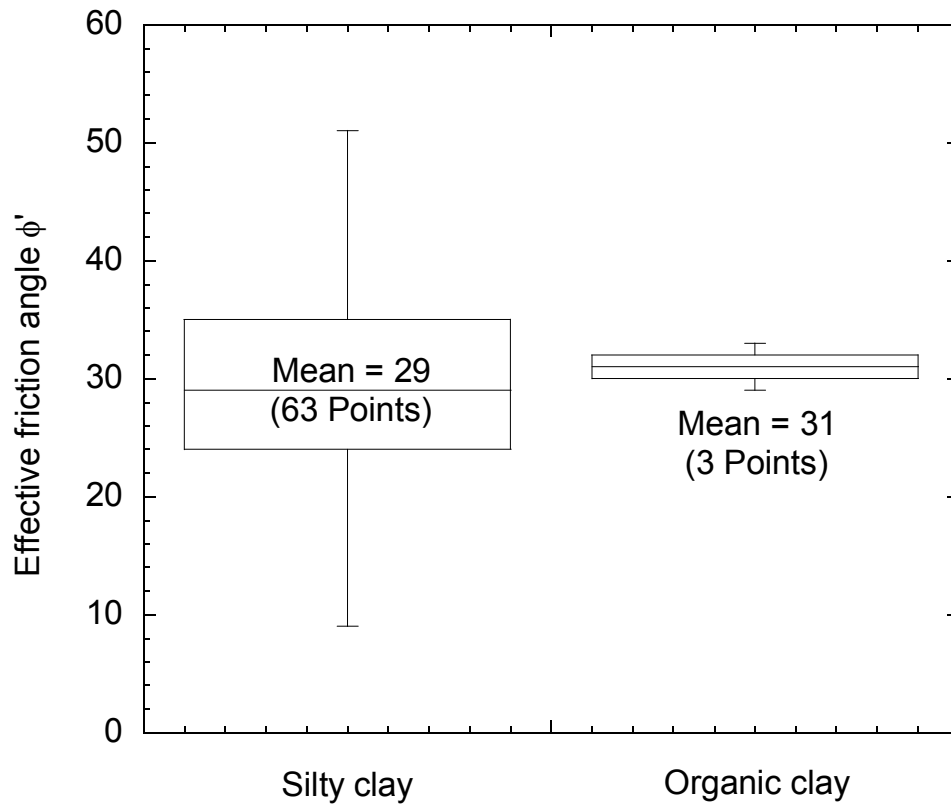


Fig. 14. Box diagram of effective friction angle (ϕ') as a function of soil type.

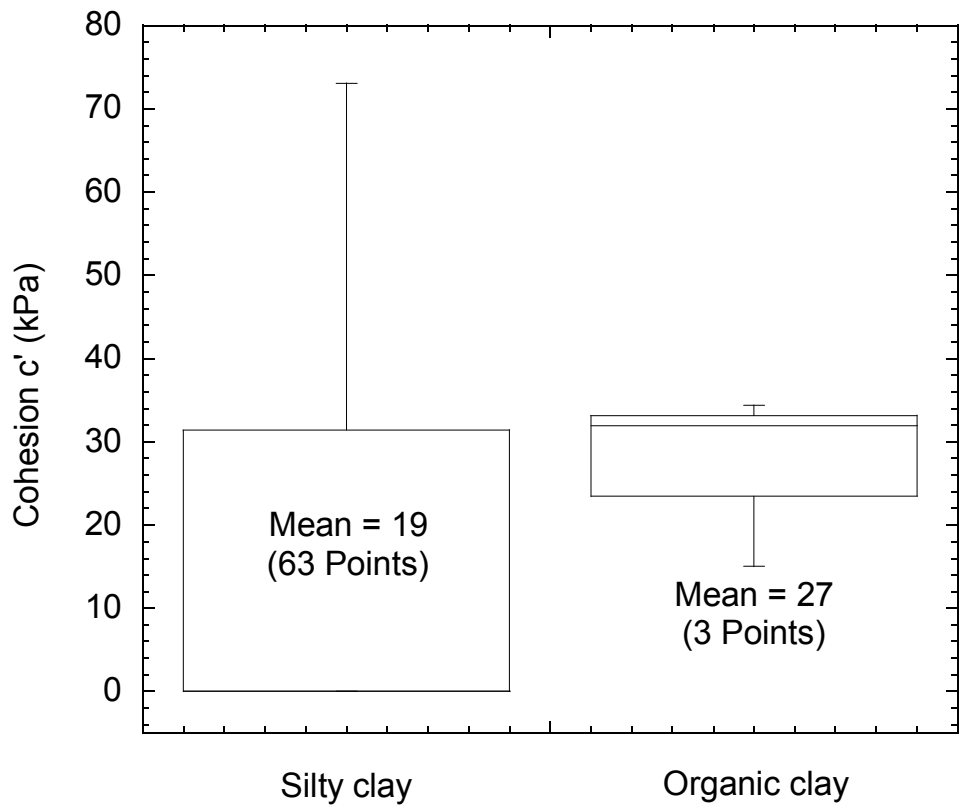


Fig. 15. Box diagram of cohesion (c') as a function of soil type.

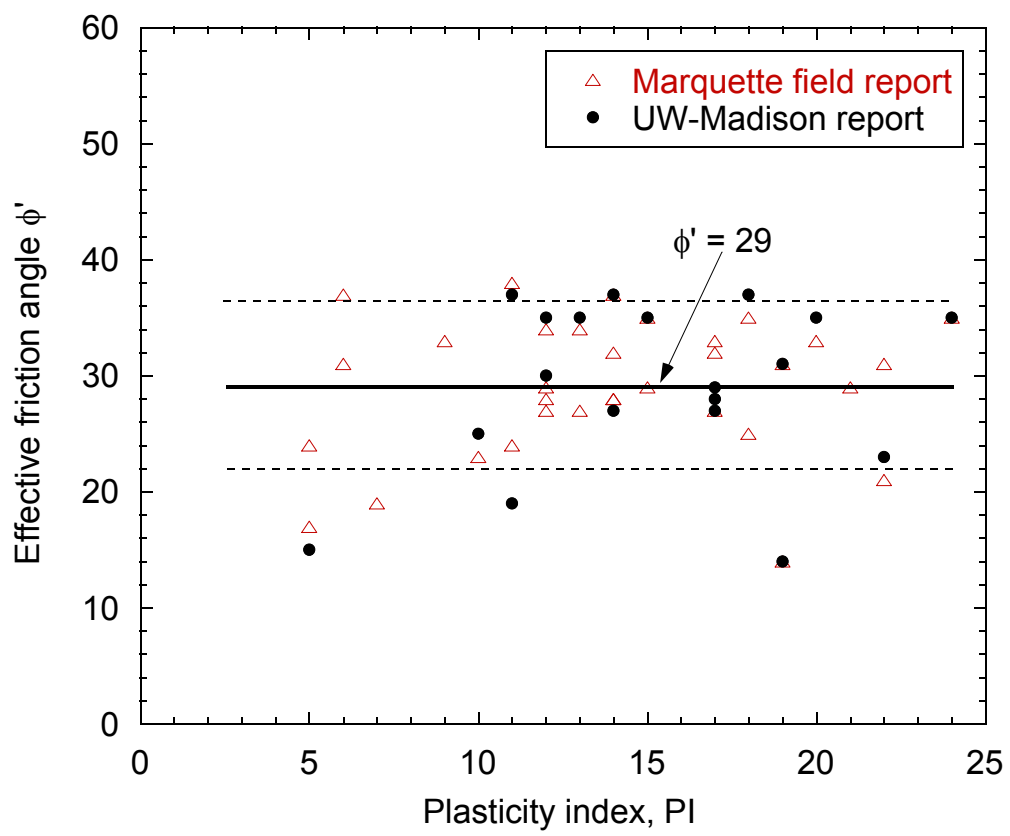


Fig. 16. Correlation between effective friction angle ϕ' and plasticity index

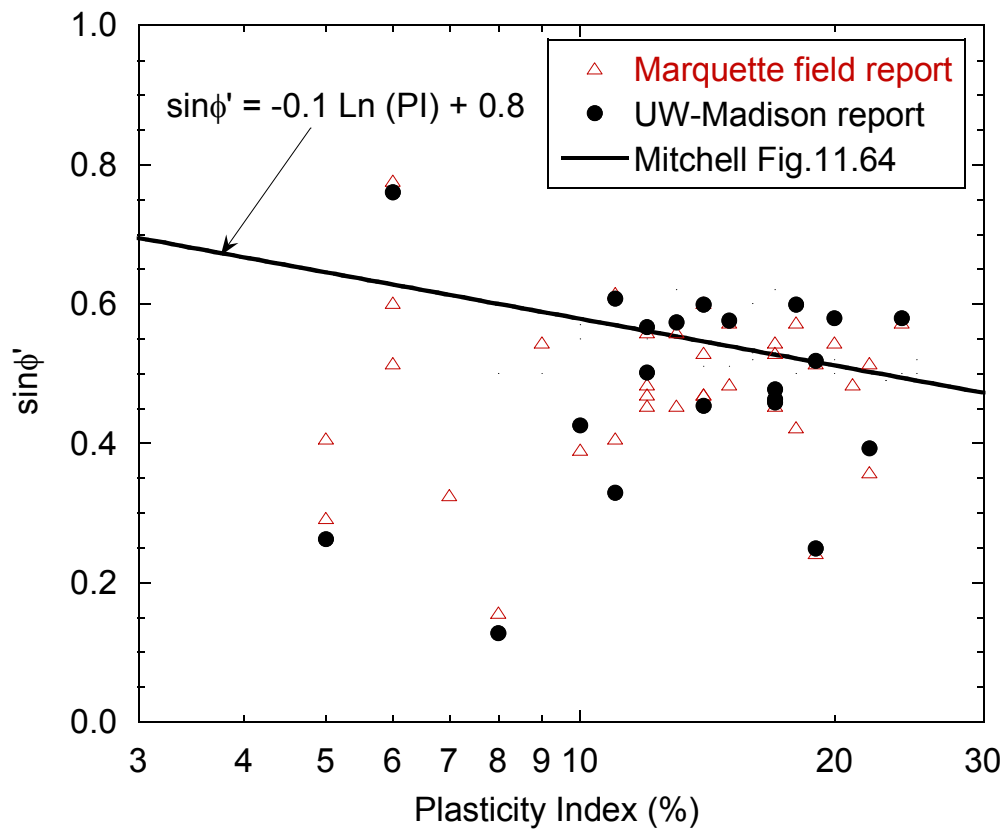


Fig. 17. Correlation between $\sin \phi'$ and plasticity index

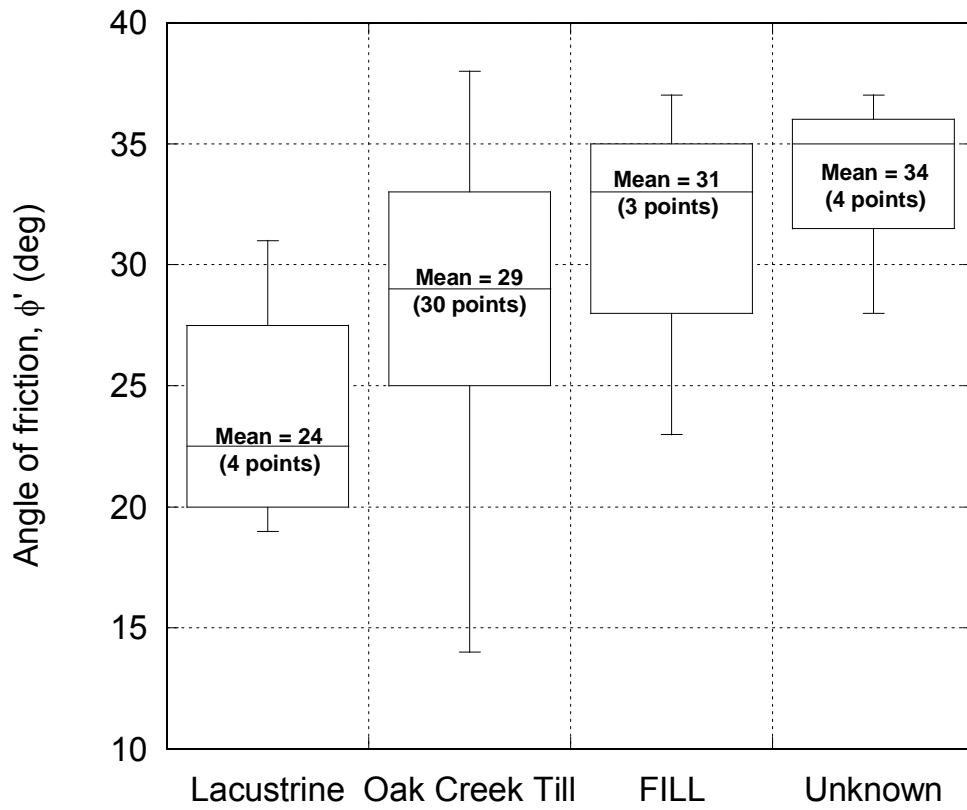


Fig. 18. Box diagram of effective angle of friction (ϕ') as a function of geological origin.

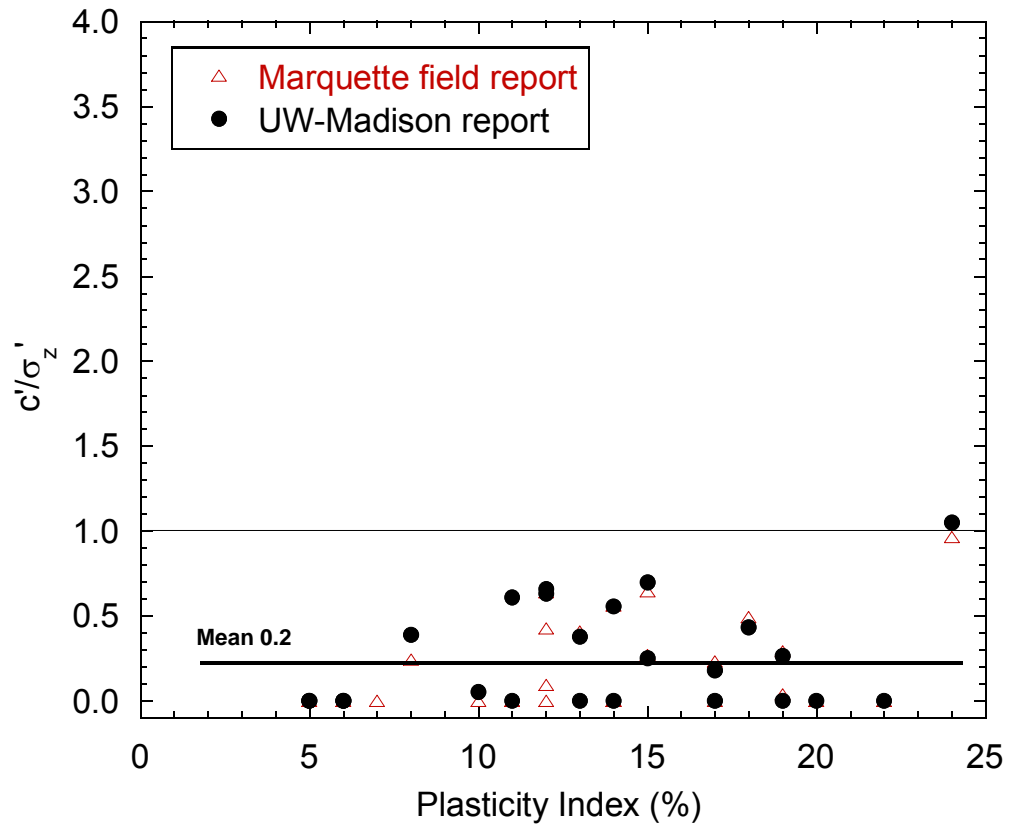


Fig. 19. Correlation between c'/σ'_z and plasticity index

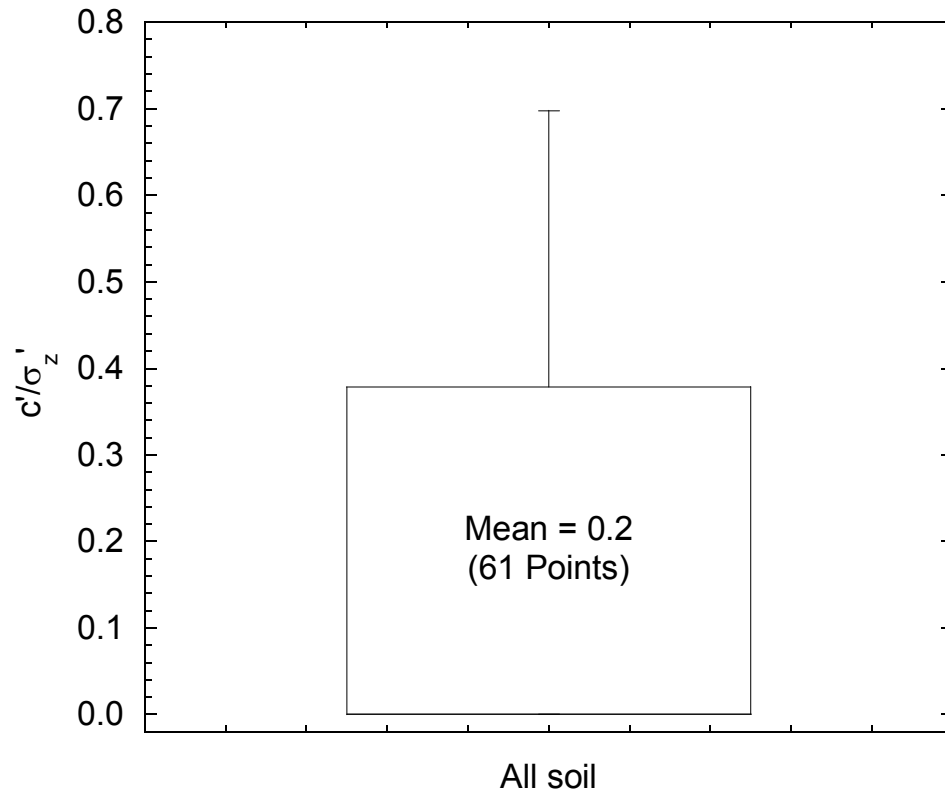


Fig. 20. Box diagram of c'/σ'_z (only 41 pairs of c'/σ'_z and the corresponding PI in Fig. 18)

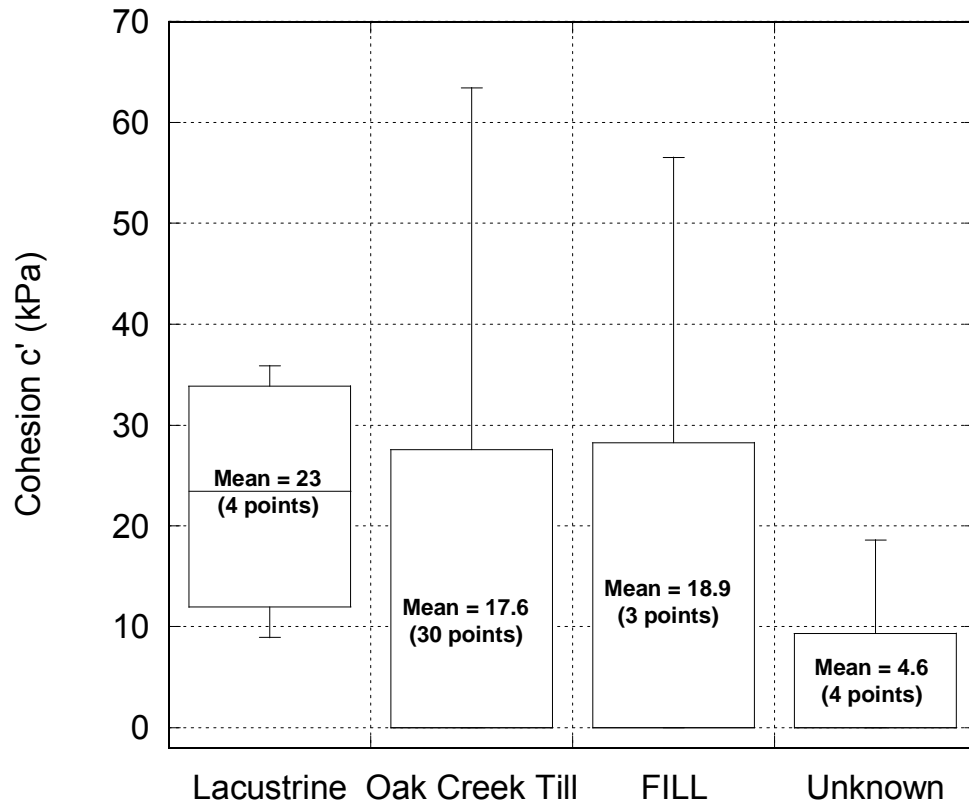


Fig. 21. Box diagram of cohesion (c') as a function of geological origin.

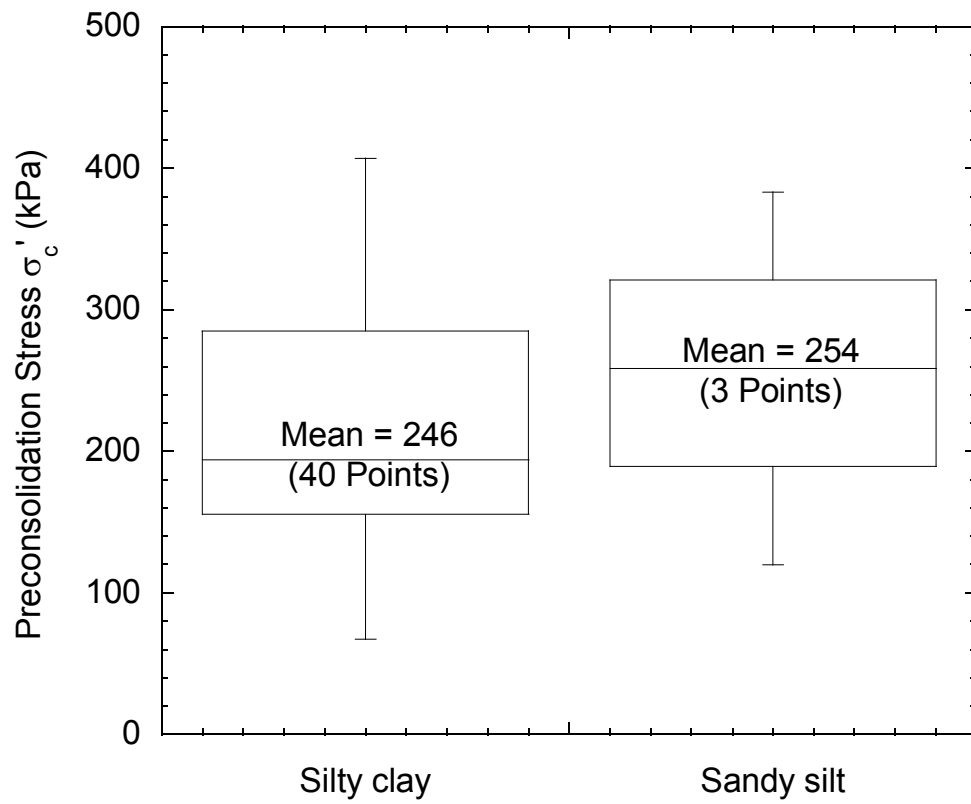


Fig. 22. Box diagram of preconsolidation stress as a function of soil type.

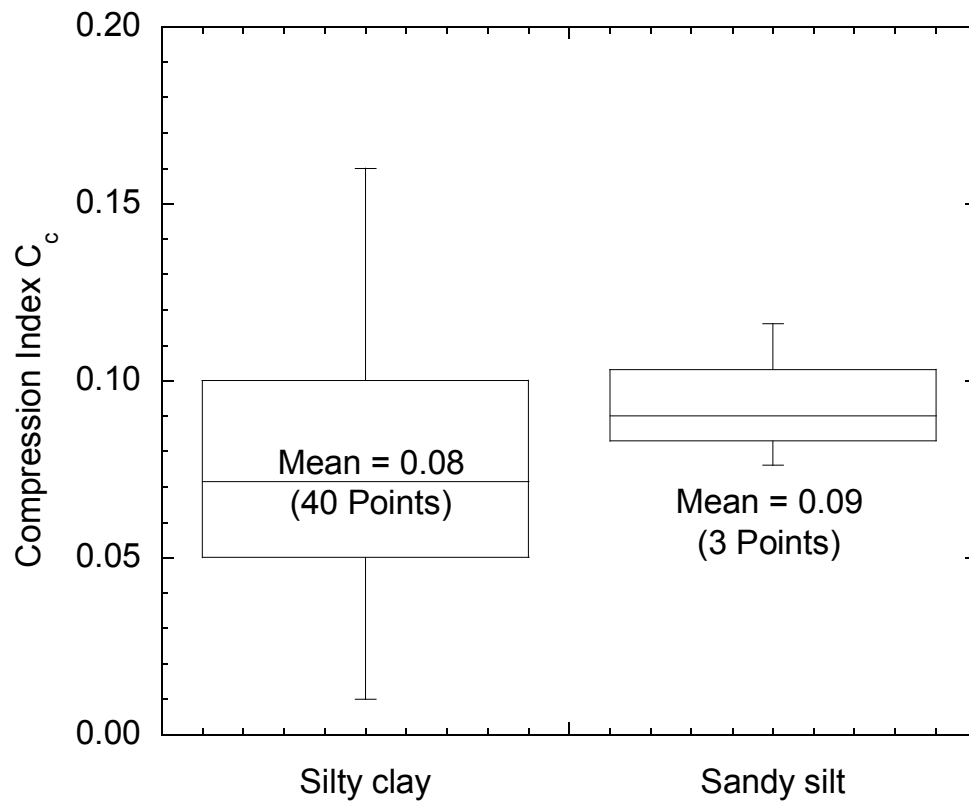


Fig. 23. Box diagram of compression index (C_c) as a function of soil type.

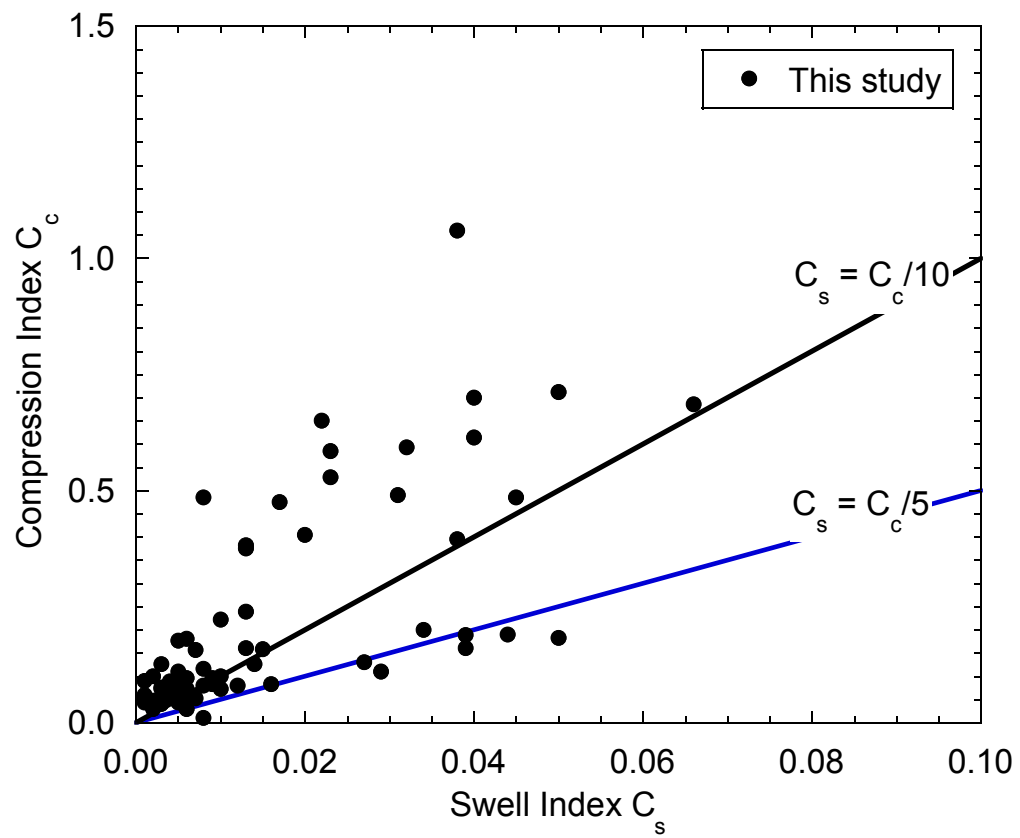


Fig. 24. Correlation between compression index and swell index.

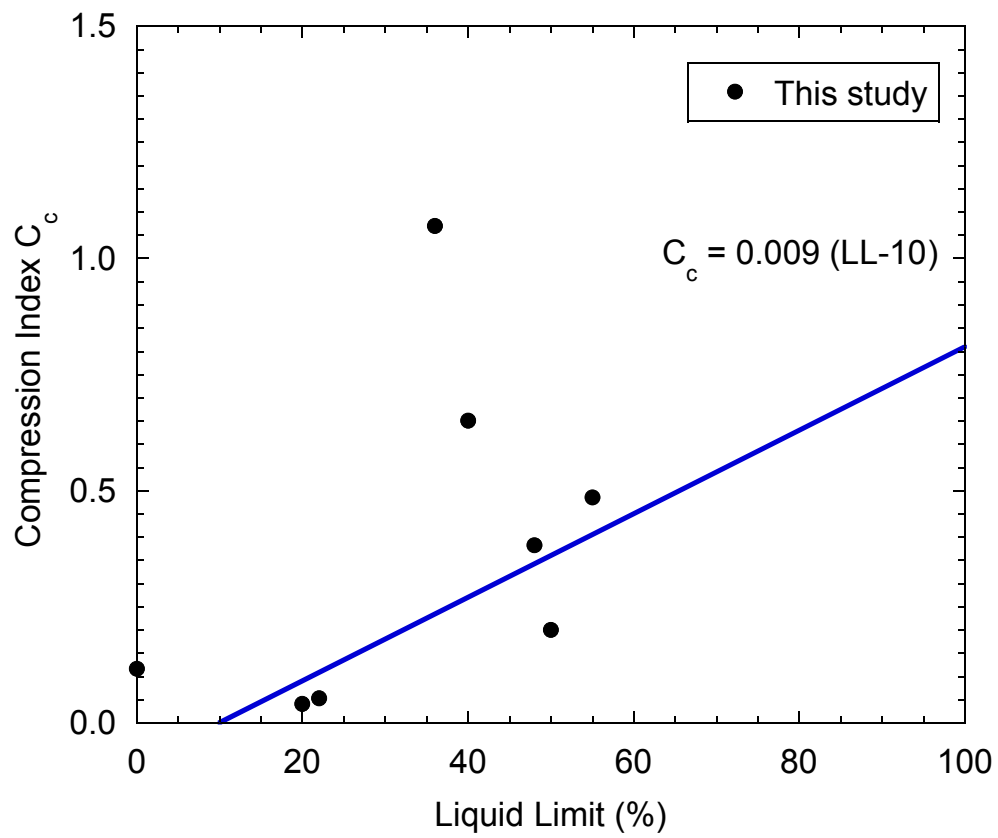


Fig. 25. Correlation between compression index and liquid limit.

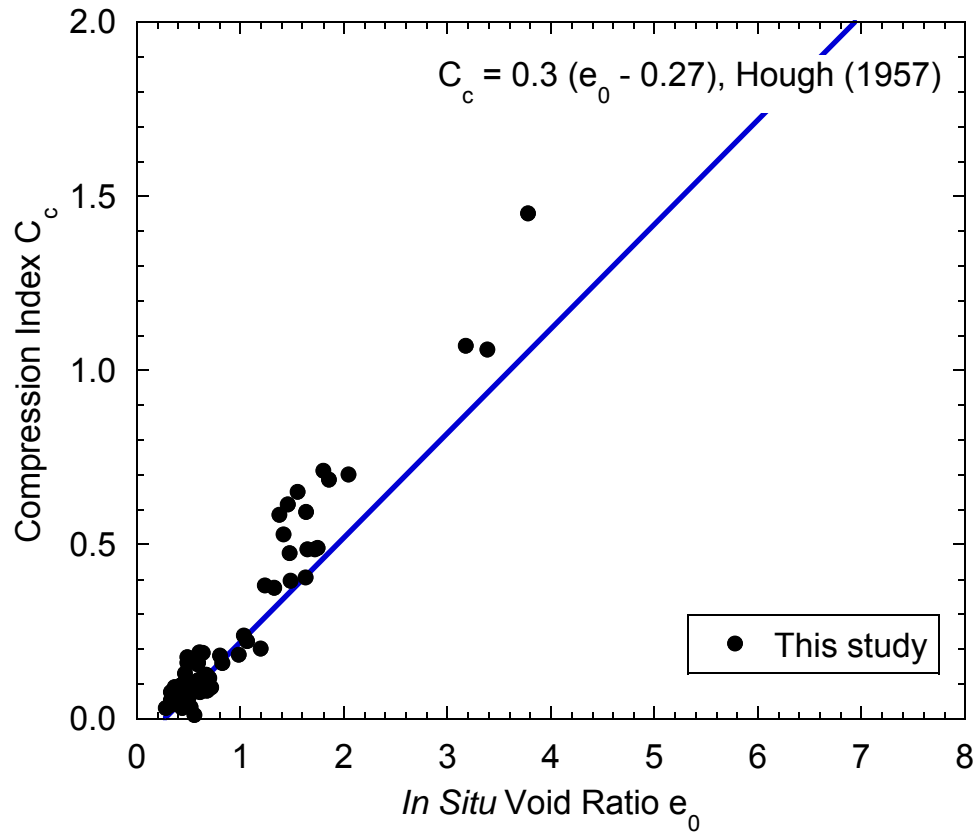


Fig. 26. Correlation between compression index and in situ void ratio.

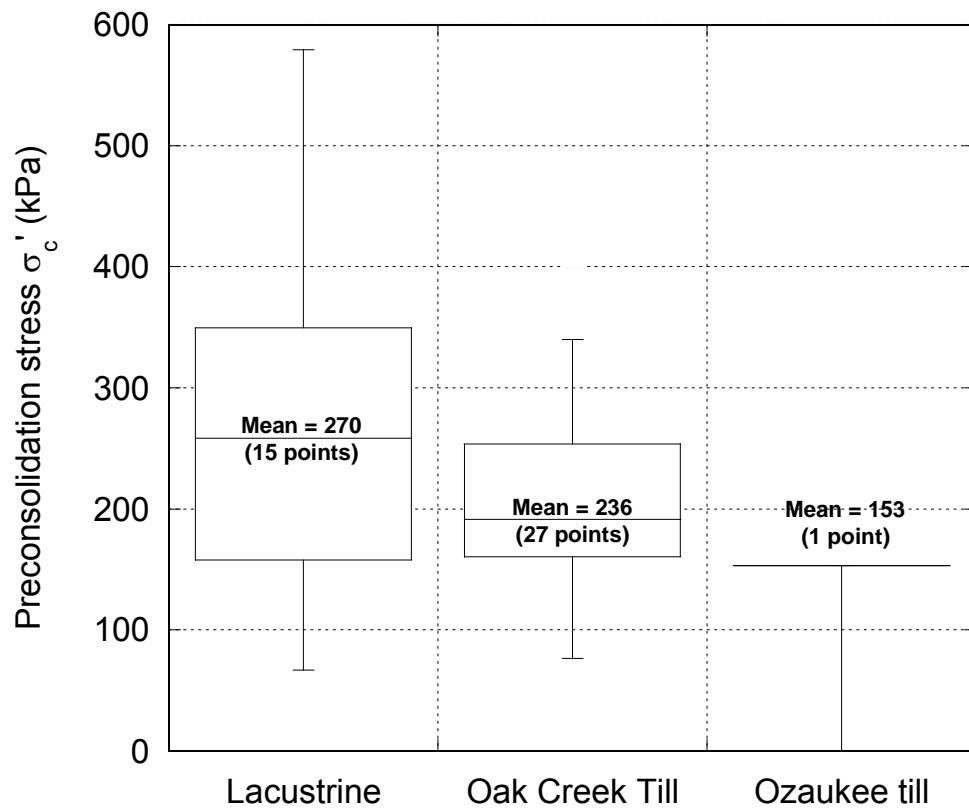


Fig. 27. Box diagram of preconsolidation stress as a function of geological origin.

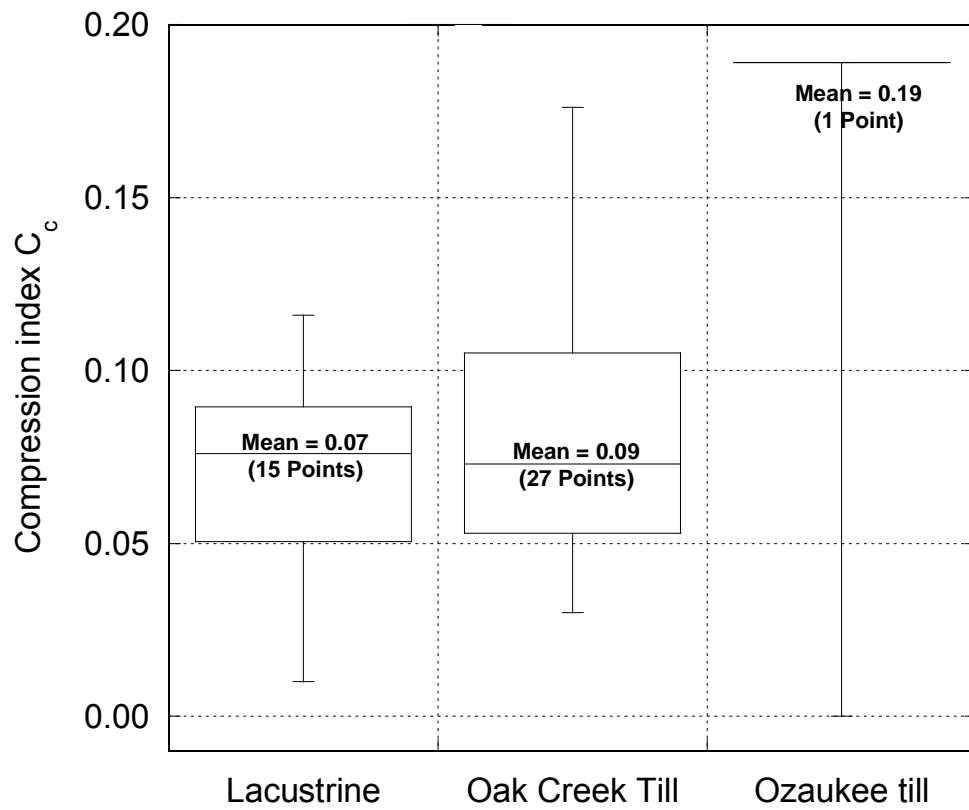


Fig. 28. Box diagram of compression index as a function of geological origin.

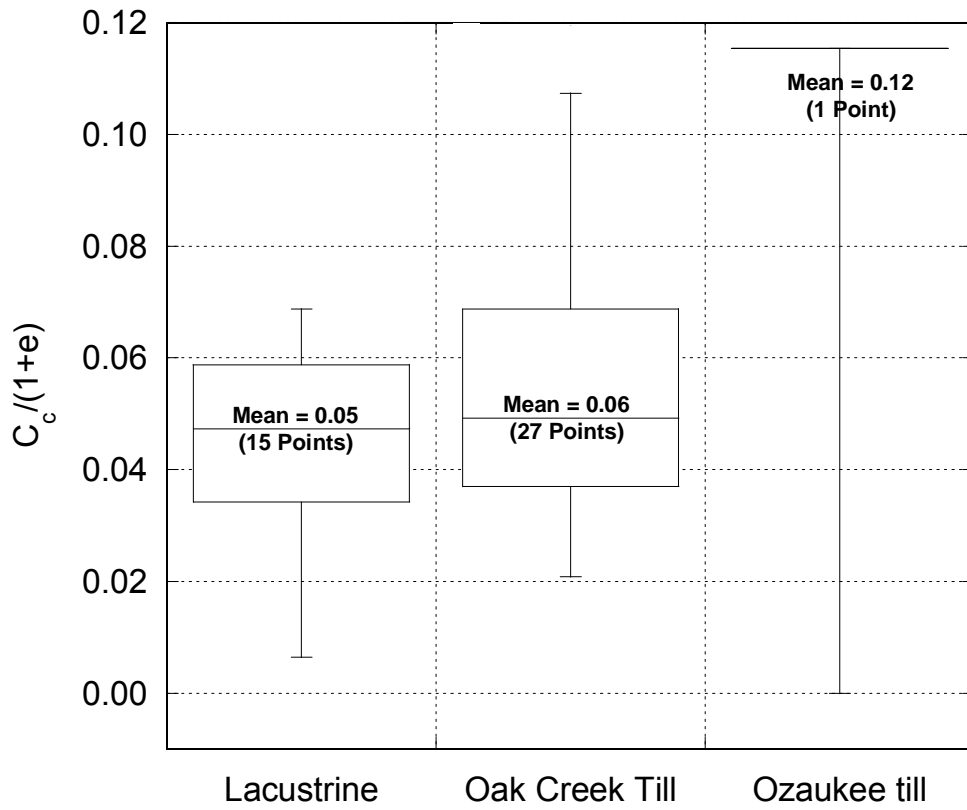


Fig. 29. Box diagram of $C_c/(1+e)$ as a function of geological origin.

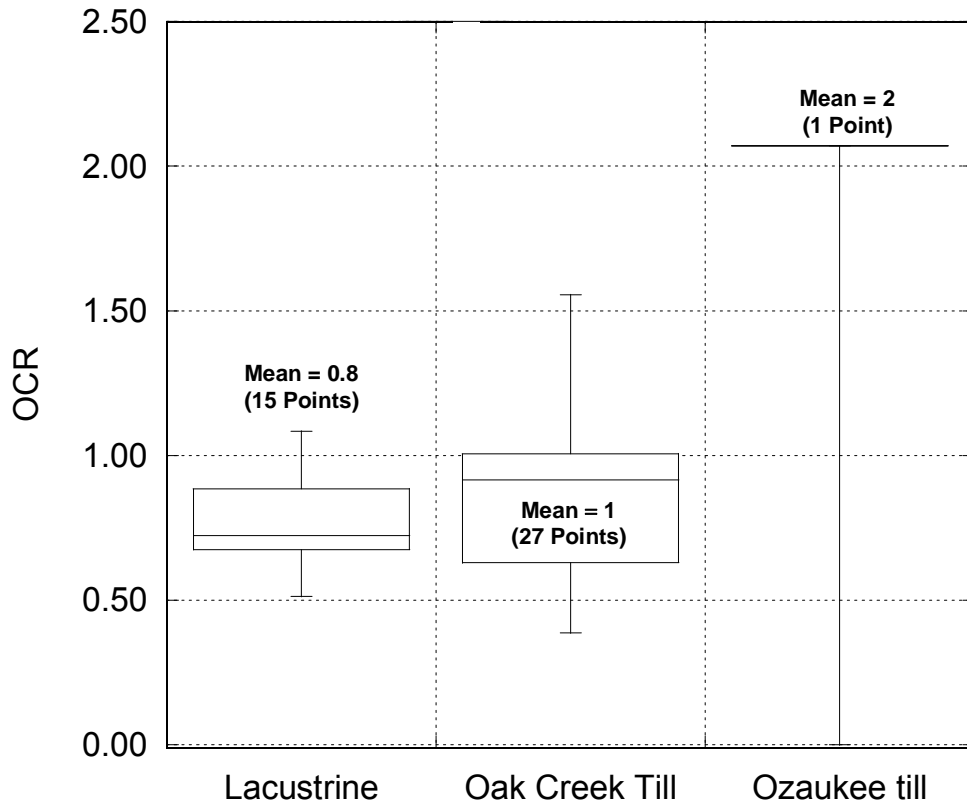


Fig. 30. Box diagram of OCR as a function of geological origin.

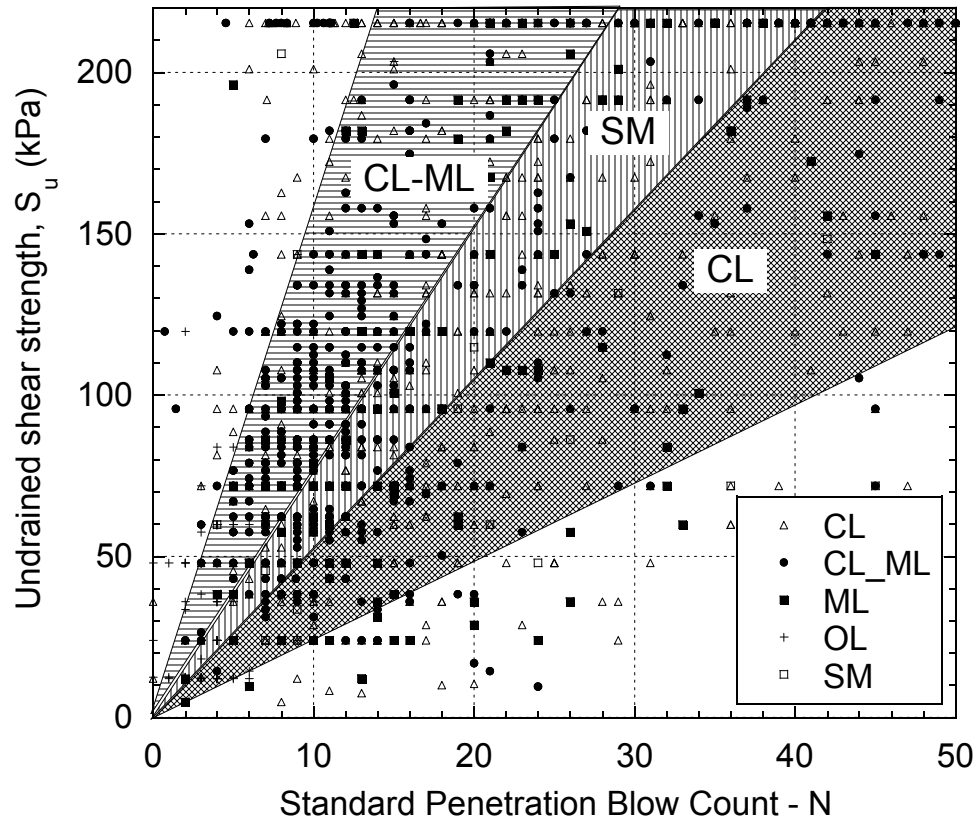


Fig. 31. Correlation between undrained shear strength and SPT-N. The undrained shear strength data are measured by pocket penetrometer.

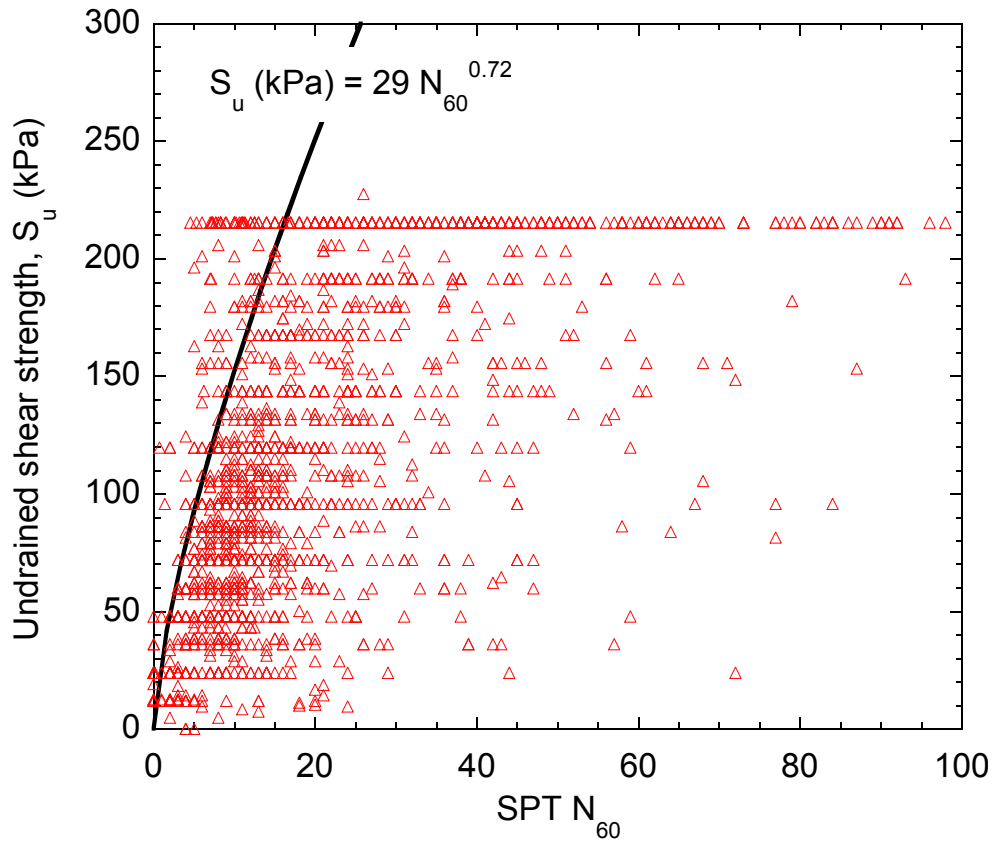


Fig. 32. Correlation between undrained shear strength and SPT- N_{60} . The undrained shear strength data are measured by pocket penetrometer.

APPENDICES